RESEARCH LETTER

AMERICAN JOURNAL OF medical genetics PART A

Prenatal Genetic Testing for a Microdeletion at Chromosome 14q32.2 Imprinted Region Leading to UPD(14)pat-like Phenotype

Aiko Sasaki,[1] Masahiro Sumie,[1] Seiji Wada,[1] Rika Kosaki,[2] Kenji Kuroswa,[3] Maki Fukami,[4] Haruhiko Sago,[1] Tsutomu Ogata,[5] and Masayo Kagami[4]*

[1]Department of Maternal-Fetal and Neonatal Medicine, National Center for Child Health and Development, Tokyo, Japan

[2]Division of Medical Genetics, National Center for Child Health and Development, Tokyo, Japan

[3]Division of Medical Genetics, Kanagawa Children's Medical Center, Yokohama, Japan

[4]Department of Molecular Endocrinology, National Research Institute for Child Health and Development, Tokyo, Japan

[5]Department of Pediatrics, Hamamatsu University School of Medicine, Hamamatsu, Japan

Manuscript Received: 17 April 2013; Manuscript Accepted: 16 July 2013

TO THE EDITOR:

Human chromosome 14q32.2 imprinted region carries several paternally expressed genes (*PEGs*) such as *DLK1* and *RTL1* and maternally expressed genes (*MEGs*) such as *MEG3* (alias, *GTL2*) and *RTL1as* (*RTL1 antisense*), together with the germline-derived primary *DLK1-MEG3* intergenic differentially methylated region (IG-DMR) and the postfertilization-derived secondary *MEG3*-DMR (Fig. 1) [da Rocha et al., 2008; Kagami et al., 2008a]. Consistent with this, paternal uniparental disomy 14 (UPD(14)) results in a unique phenotype characterized by facial abnormality, small bell-shaped thorax, abdominal wall defects, placentomegaly, and polyhydramnios [Kagami et al., 2005, 2008a,b]. In this regard, we have recently reported that heterozygous microdeletions and epimutations (hypermethylations) affecting unmethylated DMR (s) of maternal origin also lead to UPD(14)pat-like phenotype [Kagami et al., 2008a, 2010, 2012]. Indeed, after studying 26 patients with UPD(14)pat-like phenotype, we identified UPD (14)pat in 17 patients (65.4%), microdeletions in 5 patients (19.2%), and epimutations in 4 patients (15.4%) [Kagami et al., 2012]. Importantly, although there is no report describing recurrence of UPD(14)pat and epimutation in familial members with a normal karyotype, microdeletions can be transmitted recurrently from mothers with the same heterozygous microdeletions to offsprings [Kagami et al., 2008a]. Here, we report on our experience of a prenatal genetic testing for a microdeletion at the chromosome 14q32.2 imprinted region.

A 33-year-old Japanese woman came to us with her husband seeking for prenatal diagnosis of a fetus at 9 weeks of gestation. The first child and the mother have been reported previously as cases 3 and 11 of Family B in Kagami et al. [2008a]. In brief, the child had upd(14)pat-like phenotype and a maternally derived 411,354 bp microdeletion involving *WDR25*, *BEGAIN*, *DLK1*, *MEG3*, *RTL1/RTL1as*, and *MEG8* (Fig. 1). The mother had UPD(14)mat-like phenotype and the same microdeletion on the paternally derived chromosome 14. The parents hoped to deliver the fetus at a local hospital if there is no microdeletion or at our hospital with a neonatal intensive care unit if a microdeletion is identified.

After thorough consultation, we performed trans-abdominal chorionic villus sampling (CVS) at 12 weeks of gestation. Immediately after the sampling, fluorescence in situ hybridization was carried out with an RP11-566J3 probe detecting a segment within

How to Cite this Article:
Sasaki A, Sumie M, Wada S, Kosaki R, Kuroswa K, Fukami M, Sago H, Ogata T, Kagami M. 2013. Prenatal Genetic Testing for a Microdeletion at Chromosome 14q32.2 Imprinted Region Leading to UPD(14)pat-like Phenotype.
Am J Med Genet Part A 9999:1–3.

Conflict of interest: none.
Grant sponsor: Scientific Research (A); Grant numbers: 22249010, 25253023; Grant sponsor: Research (B); Grant number: 21028026; Grant sponsor: Japan Society for the Promotion of Science; Grant sponsor: Research on Intractable Diseases; Grant number: H22-161; Grant sponsor: National Center for Child Health and Development; Grant numbers: 23A-1, 25-10; Grant sponsor: Takeda Science Foundation; Grant sponsor: Novartis Foundation; Grant sponsor: The Japan and Foundation for Pediatric Research.
*Correspondence to:
Masayo Kagami, M.D, Ph.D, Department of Molecular Endocrinology, National Research Institute for Child Health and Development, Tokyo 157-8535, Japan. E-mail: kagami-ms@ncchd.go.jp
Article first published online in Wiley Online Library (wileyonlinelibrary.com): 00 Month 2013
DOI 10.1002/ajmg.a.36185

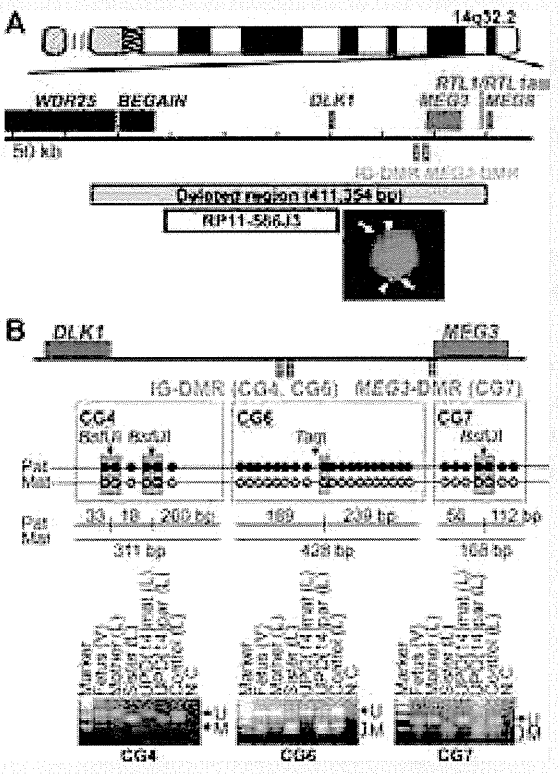

FIG. 1. Summary of the molecular studies. A: The physical map of the 14q32.2 imprinted region and the FISH finding of the fetus. *PEGs* are shown in blue, *MEGs* in red, and the IG-DMR and the *MEG3*-DMR in green. The gray rectangle indicates the 411,354 bp microdeletion identified in the first child and the mother, and the white rectangle denotes the region detected by the RP11-566J3 BAC probe. The FISH analysis reveals two red signals (arrows) identified by the RP11-566J3 BAC probe and two green signals (arrowheads) detected by the RP11-566I2 BAC probe for 14q12 utilized as an internal control. B: The methylation analysis for the IG-DMR (CG4 and CG6) and the *MEG3*-DMR (CG7) by COBRA. The black and white circles indicate methylated and unmethylated cytosines at the CpG dinucleotides, respectively. Pat: paternally derived chromosome; and Mat: maternally derived chromosome. PCR products for CG4 (311 bp) are digested with *Bst*UI into three fragments (33, 18, and 260 bp) when cytosines at the first and the second CpG dinucleotides and the fourth and fifth CpG dinucleotides (indicated with orange rectangles) are methylated. The PCR products for CG6 (428 bp) are digested with *Taq*I into two fragments (189 and 239 bp) when the cytosine at the 9th CpG dinucleotide (indicated with an orange rectangle) is methylated. The PCR products of CG7 (168 bp) are digested with *Bst*UI into two fragments (56 and 112 bp) when the cytosines at the fourth and fifth CpG dinucleotides (indicated with orange rectangle) are methylated. Both methylated (M)- and unmethylated (U)-specific bands are identified in the chorionic villus sample. V, villi; L, leukocytes; and N.C, negative control.

the deleted region of the first child and the mother, delineating two signals on villus cell interphase spreads (Fig. 1). Next combined bisulfite restriction analysis (COBRA) was performed for the IG-DMR and the *MEG3*-DMR using villus cell genomic DNA, identifying both methylated- and unmethylated allele-specific bands (Fig. 1B). These findings clearly excluded the presence of a microdeletion in the fetus by 14 weeks of gestation. Subsequent pregnant course was uneventful, and a phenotypically normal infant was delivered at term by a caesarean section.

To our knowledge, this is the first report describing a prenatal genetic testing for a familial microdeletion affecting the chromosome 14q32.2 imprinted region. Although such a genetic testing is possible only when an accurate genetic diagnosis has been made for the proband, it permitted the precise diagnosis before the second to the third trimester when characteristic UPD(14)pat-like features such as bell-shaped small thorax with coat hanger appearance and polyhydroamnios become detectable by ultrasonographic studies [Suzumori et al., 2010; Yamanaka et al., 2010]. Such an early prenatal diagnosis, though it is associated with a certain risk such as CVS-induced abortion, provides critical information for the clinical management. When a microdeletion is excluded as shown in this case, this releases the parents from the anxiety of having an affected fetus and allows for a standard follow-up during pregnancy. By contrast, when a microdeletion is identified, this will allow for appropriate management during pregnancy (e.g., amnioreduction to mitigate the risk of threatened premature delivery) and pertinent therapeutic interventions for the infant (e.g., respiratory management). Thus, prenatal genetic diagnosis appears to be beneficial for the fetus and the parents, when it is performed at appropriate institutes where a multidisciplinary team including a genetic counselor is available.

ACKNOWLEDGMENTS

This work was supported by Grants-in-Aid for Scientific Research (A) (22249010 and 25253023) and Research (B) (21028026) from the Japan Society for the Promotion of Science, by Grants for Research on Intractable Diseases (H22-161) from the Ministry of Health, Labor and Welfare (MHLW), by Grants for National Center for Child Health and Development (23A-1, 25-10), and by Grants from Takeda Science Foundation, Novartis Foundation, and The Japan and Foundation for Pediatric Research.

REFERENCES

da Rocha ST, Edwards CA, Ito M, Ogata T, Ferguson-Smith AC. 2008. Genomic imprinting at the mammalian Dlk1-Dio3 domain. Trends Genet 24:306–316.

Kagami M, Nishimura G, Okuyama T, Hayashidani M, Takeuchi T, Tanaka S, Ishino F, Kurosawa K, Ogata T. 2005. Segmental and full paternal isodisomy for chromosome 14 in three patients: Narrowing the critical region and implication for the clinical features. Am J Med Genet Part A 138A:127–132.

Kagami M, Sekita Y, Nishimura G, Irie M, Kato F, Okada M, Yamamori S, Kishimoto H, Nakayama M, Tanaka Y, Matsuoka K, Takahashi T, Noguchi M, Tanaka Y, Masumoto K, Utsunomiya T, Kouzan H, Komatsu Y, Ohashi H, Kurosawa K, Kosaki K, Ferguson-Smith AC,

Ogata T. 2008a. Deletions and epimutations affecting the human 14q32.2 imprinted region in individuals with paternal and maternal upd(14)-like phenotypes. Nat Genet 40:237–242.

Kagami M, Yamazawa K, Matsubara K, Matsuo N, Ogata T. 2008b. Placentomegaly in paternal uniparental disomy for human chromosome 14. Placenta 29:760–761.

Kagami M, O'Sullivan MJ, Green AJ, Watabe Y, Arisaka O, Masawa N, Matsuoka K, Fukami M, Matsubara K, Kato F, Ferguson-Smith AC, Ogata T. 2010. The IG-DMR and the MEG3-DMR at human chromosome 14q32.2: Hierarchical interaction and distinct functional properties as imprinting control centers. PLoS Genet 6:e1000992.

Kagami M, Kato F, Matsubara K, Sato T, Nishimura G, Ogata T. 2012. Relative frequency of underlying genetic causes for the development of UPD(14)pat-like phenotype. Eur J Hum Genet 20:928–932.

Suzumori N, Ogata T, Mizutani E, Hattori Y, Matsubara K, Kagami M, Sugiura-Ogasawara M. 2010. Prenatal findings of paternal uniparental disomy 14: Delineation of further patient. Am J Med Genet Part A 152A:3189–3192.

Yamanaka M, Ishikawa H, Saito K, Maruyama Y, Ozawa K, Shibasaki J, Nishimura G, Kurosawa K. 2010. Prenatal findings of paternal uniparental disomy 14: Report of four patients. Am J Med Genet Part A 152A:789–791.

RESEARCH LETTER

AMERICAN JOURNAL OF medical genetics PART A

Mosaic upd(7)mat in a Patient With Silver–Russell Syndrome

Tomoko Fuke-Sato,[1,2] Kazuki Yamazawa,[1] Kazuhiko Nakabayashi,[3] Keiko Matsubara,[1] Kentaro Matsuoka,[4] Tomonobu Hasegawa,[2] Kazushige Dobashi,[5] and Tsutomu Ogata[1,6]*

[1]Department of Molecular Endocrinology, National Research Institute for Child Health and Development, Tokyo, Japan

[2]Department of Pediatrics, Keio University School of Medicine, Tokyo, Japan

[3]Department of Maternal-Fetal Biology, National Research Institute for Child Health and Development, Tokyo, Japan

[4]Division of Pathology, National Medical Center for Children and Mothers, Tokyo, Japan

[5]Department of Pediatrics, Showa University School of Medicine, Tokyo, Japan

[6]Department of Pediatrics, Hamamatsu University School of Medicine, Hamamatsu, Japan

Received 10 March 2011; Accepted 9 November 2011

TO THE EDITOR:

Silver–Russell syndrome (SRS) is a congenital developmental disorder characterized by pre- and post-natal growth failure, relative macrocephaly, triangular face, hemihypotrophy, and 5th finger clinodactyly [Russell, 1954; Silver et al., 1953]. Recent studies have shown that hypomethylation (epimutation) of the paternally derived differentially methylated region (DMR) in the upstream of *H19* (*H19*-DMR) on chromosome 11p15 and maternal uniparental disomy for chromosome 7 (upd(7)mat) account for ~45% and ~5–10% of SRS patients, respectively [Eggermann, 2010; Binder et al., 2011]. Furthermore, consistent with the involvement of imprinted genes in both body and placental growth [for review, Coan et al., 2005], epimutations of the *H19*-DMR and upd(7)mat are known to result in placental hypoplasia [Yamazawa et al., 2008a,b]. Here, we report on a Japanese boy with mosaic upd(7)mat who was identified through genetic screenings in 120 patients with SRS-like phenotype.

This Japanese boy was conceived naturally to a 41-year-old father and a 36-year-old mother. The parents were non-consanguineous and healthy. The paternal height was 165 cm (−0.9 SD), and the maternal height 155 cm (−0.6 SD).

At 35 weeks of gestation, he was delivered by a cesarean because of fetal distress. At birth, his length was 37.4 cm (−3.1 SD), his weight 1.28 kg (−3.1 SD), and his head circumference 29.0 cm (−1.3 SD). The placenta weighed 400 g (−0.6 SD [Kagami et al., 2008]). Shortly after birth, he was found to have ventricular septal defect, hydronephrosis, and abnormal external genitalia (hypospadias, bifid scrotum, and bilateral cryptorchidism). He received orchidopexy at $1^{10}/_{12}$ years of age and genitoplasty at $2^{4}/_{12}$ years of age. He exhibited feeding difficulty and speech delay.

At $5^{1}/_{12}$ years of age, he was referred because of short stature. His height was 87.9 cm (−4.3 SD), weight was 10.4 kg (−2.9 SD), and his head circumference 49.0 cm (−0.7 SD). Physical examination showed relative macrocephaly, abnormal teeth, 5th finger clinodactyly, and underdeveloped muscles. There was no hemihypotrophy. Endocrine studies for short stature yielded normal results, as did radiological examinations. His karyotype was 46,XY in all the 50 lymphocytes examined. He was clinically diagnosed as having SRS, and molecular studies were performed after obtaining the approval from the Institutional Review Board Committee at National Center for Child Health and Development and the written informed consent from the parents.

We first performed methylation analysis of the *MEST*-DMR on chromosome 7q32.2 using leukocyte genomic DNA by the previously described methods [Yamazawa et al., 2008b], because this patient showed relatively mild SRS-phenotype with speech delay

How to Cite this Article:
Fuke-Sato T, Yamazawa K, Nakabayashi K, Matsubara K, Matsuoka K, Hasegawa T, Dobashi K, Ogata T. 2012. Mosaic upd(7)mat in a patient with Silver–Russell syndrome. Am J Med Genet Part A 158A:465–468.

Grant sponsor: Japan Society for the Promotion of Science (JSPS); Grant number: 22249010; Grant sponsor: Ministry of Health, Labor and Welfare; Grant number: H21-005; Grant sponsor: Grant of National Center for Child Health and Development; Grant number: 23A-1.

*Correspondence to:
Tsutomu Ogata, M.D., Department of Pediatrics, Hamamatsu University School of Medicine, Hamamatsu 431-3192, Japan.
E-mail: tomogata@hama-med.ac.jp

Published online 13 January 2012 in Wiley Online Library (wileyonlinelibrary.com).
DOI 10.1002/ajmg.a.34404

and feeding difficulty characteristic of upd(7)mat [Hitchins et al., 2001; Kotzot, 2008]. The methylation analysis showed a major peak for methylated clones and a minor peak for unmethylated clones in this patient (Fig. 1A). We also examined the *H19*-DMR and other multiple DMRs on various chromosomes by the bio-COBRA (combined bisulfite restriction analysis) method, as reported previously [Yamazawa et al., 2010]. The *GRB10*-DMR on chromosome 7p12.1 and the *PEG10*-DMR on chromosome 7q21.3 exhibited skewed methylation patterns consistent with the predominance of maternally derived clones, as did the *MEST*-DMR (Fig. 1B). By

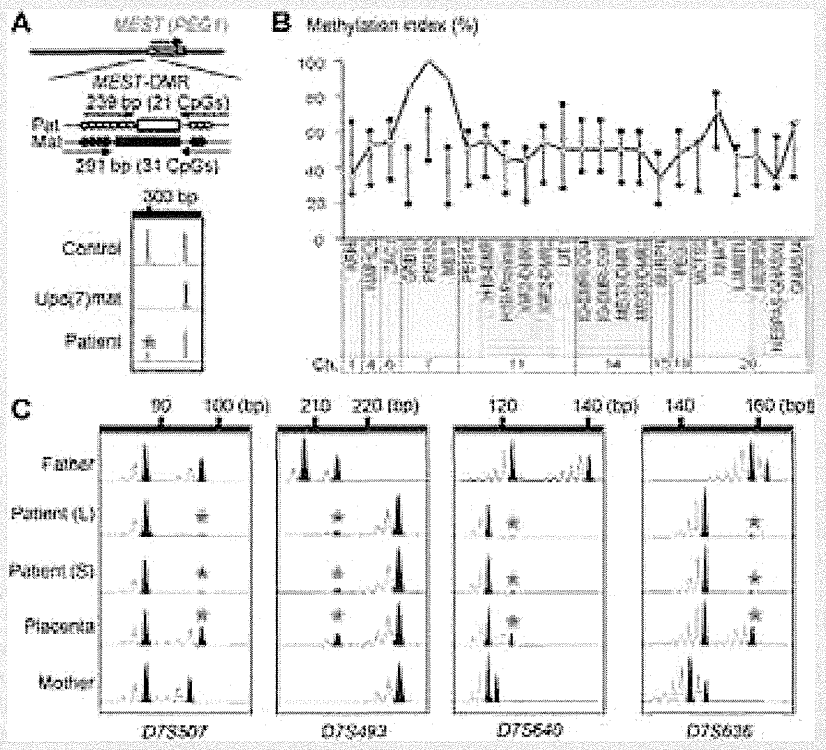

FIG. 1. Representative molecular results. A: Methylation analysis for the *MEST*-DMR. The methylated and unmethylated allele-specific primers were designed to yield PCR products of different sizes, and the PCR products were visualized on the 2100 Bioanalyzer (Agilent, Santa Clara, CA). Both methylated and unmethylated alleles are amplified in a control subject, and the methylated allele only is identified in a previously reported patient with upd(7)mat [Yamazawa et al., 2008b]. In this patient, a major peak for the methylated allele and a minor peak for the unmethylated allele (a red asterisk) are delineated. B: Methylation indices of 24 DMRs examined by the bio-COBRA. The PCR products were digested with methylation sensitive restriction enzymes, and the methylation indices (the ratios of methylated clones) were calculated using peak heights of digested and undigested fragments on the 2100 Bioanalyzer using 2100 expert software. The black vertical bars indicate the reference data in 20 normal control subjects (maximum − minimum). The DMRs highlighted in blue and pink are methylated after paternal and maternal transmissions, respectively.
C: Microsatellite analysis. Major peaks of maternal origin and minor peaks of paternal origin (red asterisks) are identified in this patient. The minor peaks of paternal origin are more obvious in the placenta than in the leukocytes (L) and salivary cells (S). Calculation of the mosaic ratio using the *D7S507* data, under the assumption of no trisomic cells. For this locus, the patient is considered to be heterozygous with the major 87 bp peak of maternal origin and a minor 97 bp peak of paternal origin. The father is also heterozygous with the two peaks of the same sizes, and the area under curve (AUC) is larger for the short 87 bp peak than for the long 97 bp peak. This unequal amplification is consistent with short products being more easily amplified than long products. In this patient, the AUC ratio between the major 87 bp peak and the minor 97 bp peak is obtained as 1.0:0.043 for leukocytes, 1.0:0.044 for salivary cells, and 1.0:0.803 in placental tissue, after compensation of the unequal amplification between the two peaks using the paternal data. Here, let "XL" represent the frequency of the upid(7)mat cells in leukocytes (thus, (1 − XL) denotes the frequency of normal cells in leukocytes). Then, the paternally derived 97 bp peak is generated by one paternally derived chromosome in the normal cells, that is, (1 − XL), and the maternally derived 87 bp peak is formed by the products from two maternally derived homologous chromosomes in the upid(7)mat cells and one maternally derived chromosome in the normal cells, that is, $\{2XL + (1 - XL)\} = (XL + 1)$. Thus, the AUC ratio between the two peaks is represented as $(XL + 1):(1 - XL) = 1.0:0.043$, and "XL" is calculated as 0.92 (92%). Similarly, when "XS" and "XP" represent the frequency of the upid(7)mat cells in salivary cells and placental tissue, respectively, "XS" is obtained as 0.91 (91%) and "XP" as 0.11 (11%). Furthermore, when "XB" represents the frequency of the upid(7)mat cells in buccal epithelium cells, "XB" is obtained as 0.91 (91%), on the basis of the previous report that salivary cells comprises ~40% of buccal epithelium cells and ~60% of leukocytes [Thiede et al., 2000].

TABLE I. The Results of Microsatellite Analysis

Locus	Position	Father	Patient (L)	Patient (S)	Placenta	Mother	Assessment
D7S517	7p22.2	254/258	(254)/258	(254)/258	(254)/258	256/258	Maternal Iso-D[a]/biparental
D7S507	7p15–21	87/97	87/(97)	87/(97)	87/(97)	87/95	Maternal Iso-D[a]/biparental
D7S493	7p15.3	208/214	(214)/226	(214)/226	(214)/226	226	Maternal D[b]/biparental
D7S484	7p14–15	96/100	(96)/98	(96)/98	(96)/98	98/100	Maternal Iso-D/biparental
D7S502	7q11.12	298	294/(298)	294/(298)	294/(298)	294/304	Maternal Iso-D/biparental
D7S669	7q11.2	116/126	(116)/124	(116)/124	(116)/124	124	Maternal D[b]/biparental
D7S515	7q21–22	169/173	171/(173)	171/(173)	171/(173)	169/171	Maternal Iso-D/biparental
D7S640	7q21.1–31.2	122/140	116/(122)	116/(122)	116/(122)	116/118	Maternal Iso-D/biparental
D7S684	7q34	169/179	177/(179)	177/(179)	177/(179)	177/179	Not informative
D7S636	7q35–36	158/162	146/(158)	146/(158)	146/(158)	142/146	Maternal Iso-D/biparental
D7S798	7q36	73/79	(79)/83	(79)/83	(79)/83	73/83	Maternal Iso-D/biparental

L, leukocytes; S, salivary cells; D, disomy.
The Arabic numbers denote the PCR product sizes in bp.
The minor peaks are indicated in parentheses.
[a]On the basis of the results of other informative loci, the major peaks are considered to be of maternal origin.
[b]Because of the maternal homozygosity, disomic status (isodisomy or heterodisomy) is unknown for these loci.

contrast, other DMRs including the *H19*-DMR showed normal methylation patterns.

We next performed microsatellite analysis for 11 loci on various parts of chromosome 7, using genomic DNA from leukocytes of the patient and the parents, from salivary cells of the patient, and from formalin-fixed and paraffin-embedded placental tissue. Major peaks consistent with maternal uniparental isodisomy and minor peaks of paternal origin were unequivocally identified for *D7S484*, *D7S502*, *D7S515*, *D7S640*, *D7S636*, and *D7S798*; furthermore, similar patterns were also detected for *D7S517*, *D7S507*, *D7S669*, and *D7S493*, although the results were not informative for *D7S684* (Fig. 1C and Table I). The minor peaks of paternal origin were similar between leukocytes and salivary cells and more evident in placental tissue. These findings, together with the normal karyotype in lymphocytes, indicated mosaic full maternal isodisomy for chromosome 7 (upid(7)mat) in this patient. Furthermore, since such a condition is frequently associated with mosaicism for trisomy 7 [Petit et al., 2011], we performed fluorescence in situ hybridization (FISH) analysis for stocked lymphocyte pellets, using a CEP7 probe for *D7Z1* (Abbott Laboratories, Abbott Park, IL). The FISH analysis identified two normal signals in 995 of 1,000 interphase nuclei examined, with no trace of trisomic nuclei; while a single signal was delineated in the remaining five nuclei, this was regarded as a false-positive finding. Thus, assuming no trisomic cells, the frequency of the full upid(7)mat cells was calculated as 92% in leukocytes, using the results of *D7S507* (Fig. 1C). In addition, similarly assuming no trisomic cells in other tissues, the frequency of the full upid(7)mat cells was calculated as 91% salivary cells (and in buccal cells) and 11% in placental tissue, although we could not perform FISH analysis in buccal cells and placental cells.

These results imply that this patient had an abnormal cell lineage with full upid(7)mat and a normal cell lineage with biparentally inherited chromosome 7 homologs at least in lymphocytes, and these had no trisomy 7. It is likely that mitotic non-disjunction and subsequent trisomy rescue (loss of the paternally derived chromosome 7 from a trisomic cell) took place in the post-zygotic developmental stage, resulting in the production of the mosaic full upid(7)mat (Fig. 2). While full upid(7)mat can also be produced by monosomy rescue (duplication of a single maternally derived chromosome 7 in a zygote), this mechanism is predicted to cause non-mosaic rather than mosaic upid(7)mat [Miozzo et al., 2001]. Although it remains to be clarified why trisomic cells mediating the production of full upid(7)mat cells were apparently absent in lymphocytes of this patient, there might be a negative selection against lymphocytes with trisomy 7.

However, the presence or absence of demonstrable trisomic cells was studied only in lymphocytes. In this regard, trisomic cells have been identified more frequently in skin fibroblasts and amniocytes than in blood cells in patients with mosaic trisomy 7 [Chen et al., 2010; Petit et al., 2011], and they are usually more frequently detected in the placental tissue than in the body tissue, as has been demonstrated by confined placental trisomy [Kalousek et al., 1991]. These findings would argue for the possible presence of trisomic cells in several tissues including placenta of this patient.

The full upid(7)mat cells were assessed to account for the majority of the leukocytes and salivary cells (buccal cells) and the minority of the placental tissue, under the assumption of no

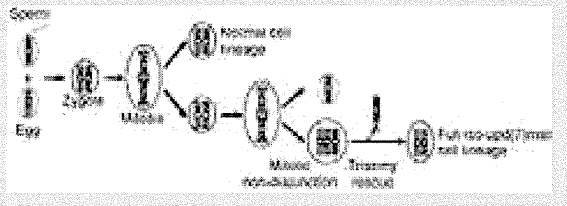

FIG. 2. Schematic representation of the generation of the mosaic upid(7)mat. The maternally and paternally derived chromosome 7 homologs are shown in red and blue, respectively. In this figure, mitotic non-disjunction is assumed at the second mitosis.

trisomic cells. In this regard, if trisomic cells may be present in a certain fraction of buccal cells and placental tissue, the full upid(7)mat cells would still account for a relatively major fraction of buccal cells and a relatively minor fraction of the placental cells. While such a variation in the frequency of the full upid(7)mat cells among different tissues would primarily be a stochastic event, it should be pointed out that human genetic studies are usually performed for leukocytes. Indeed, if the upid(7)mat cells were barely present in leukocytes, the mosaic upid(7)mat would not have been detected. Such a bias in human studies would more or less be relevant to the relative predominance of the full upid(7)mat cells in leukocytes.

Two findings are noteworthy with regard to clinical features of this patient. First, this patient had relatively mild SRS phenotype with speech delay and feeding difficulty. Since such clinical features are grossly consistent with those of patients with upd(7)mat [Hitchins et al., 2001; Kotzot, 2008], it is inferred that the upid(7)mat cells accounted for a considerable fraction of body cells relevant to the development of SRS phenotype. Second, the placental size remained within the normal range. This would be consistent with the relative paucity of the upid(7)mat cells in the placenta.

In summary, we observed mosaic upid(7)mat in a patient with SRS. Further studies will identify mosaic upd(7)mat with or without demonstrable trisomy 7 in patients with relatively mild SRS-like phenotype.

ACKNOWLEDGMENTS

This work was supported by the Grant-in-Aid for Scientific Research (A) (22249010) from the Japan Society for the Promotion of Science (JSPS), by the Grants for Health Research on Children, Youth, and Families (H21-005) from the Ministry of Health, Labor and Welfare, and by the Grant of National Center for Child Health and Development (23A-1).

REFERENCES

Binder G, Begemann M, Eggermann T, Kannenberg K. 2011. Silver-Russell syndrome. Best Pract Res Clin Endocrinol Metab 25:153–160.

Chen CP, Su YN, Chern SR, Hwu YM, Lin SP, Hsu CH, Tsai FJ, Wang TY, Wu PC, Lee CC, Chen YT, Chen LF, Wang W. 2010. Mosaic trisomy 7 at amniocentesis: Prenatal diagnosis and molecular genetic analyses. Taiwan J Obstet Gynecol 49:333–340.

Coan PM, Burton GJ, Ferguson-Smith AC. 2005. Imprinted genes in the placenta: A review. Placenta 26:S10–S20.

Eggermann T. 2010. Russell–Silver syndrome. Am J Med Genet Part C 154C:355–364.

Hitchins MP, Stanier P, Preece MA, Moore GE. 2001. Silver-Russell syndrome: A dissection of the genetic aetiology and candidate chromosomal regions. J Med Genet 38:810–819.

Kagami M, Yamazawa K, Matsubara K, Matsuo N, Ogata T. 2008. Placentomegaly in paternal uniparental disomy for human chromosome 14. Placenta 29:760–761.

Kalousek DK, Howard-Peebles PN, Olson SB, Barrett IJ, Dorfmann A, Black SH, Schulman JD, Wilson RD. 1991. Confirmation of CVS mosaicism in term placentae and high frequency of intrauterine growth retardation association with confined placental mosaicism. Prenat Diagn 11:743–750.

Kotzot D. 2008. Maternal uniparental disomy 7 and Silver–Russell syndrome—Clinical update and comparison with other subgroups. Eur J Med Genet 51:444–451.

Miozzo M, Grati FR, Bulfamante G, Rossella F, Cribiù M, Radaelli T, Cassani B, Persico T, Cetin I, Pardi G, Simoni G. 2011. Post-zygotic origin of complete maternal chromosome 7 isodisomy and consequent loss of placental *PEG1/MEST* expression. Placenta 22:813–821.

Petit F, Holder-Espinasse M, Duban-Bedu B, Bouquillon S, Boute-Benejean O, Bazin A, Rouland V, Manouvrier-Hanu S, Delobel B. 2011. Trisomy 7 mosaicism prenatally misdiagnosed and maternal uniparental disomy in a child with pigmentary mosaicism and Russell–Silver syndrome. Clin Genet [Epub ahead of print], PHID: 21204802.

Russell A. 1954. A syndrome of intra-uterine dwarfism recognizable at birth with cranio-facial dysostosis, disproportionately short arms and other anomalies. Proc R Soc Med 47:1040–1044.

Silver HK, Kiyasu W, George J, Deamer WC. 1953. Syndrome of congenital hemihypertrophy, shortness of stature, and elevated urinary gonadotrophins. Pediatrics 12:368–375.

Thiede C, Prange-Krex G, Freiberg-Richter J, Bornhäuser M, Ehninger G. 2000. Buccal swabs but not mouthwash samples can be used to obtain pretransplant DNA fingerprints from recipients of allogeneic bone marrow transplants. Bone Marrow Transplant 25:575–577.

Yamazawa K, Kagami M, Nagai T, Kondoh T, Onigata K, Maeyama K, Hasegawa T, Hasegawa Y, Yamazaki T, Mizuno S, Miyoshi Y, Miyagawa S, Horikawa R, Matsuoka K, Ogata T. 2008a. Molecular and clinical findings and their correlations in Silver-Russell syndrome: Implications for a positive role of IGF2 in growth determination and differential imprinting regulation of the *IGF2-H19* domain in bodies and placentas. J Mol Med 86:1171–1181.

Yamazawa K, Kagami M, Ogawa M, Horikawa R, Ogata T. 2008b. Placental hypoplasia in maternal uniparental disomy for chromosome 7. Am J Med Genet Part A 146A:514–516.

Yamazawa K, Nakabayashi K, Kagami M, Sato T, Saitoh S, Horikawa R, Hizuka N, Ogata T. 2010. Parthenogenetic chimaerism/mosaicism with a Silver-Russell syndrome-like phenotype. J Med Genet 47:782–785.

OPEN ACCESS Freely available online

PLOS ONE

Molecular and Clinical Studies in 138 Japanese Patients with Silver-Russell Syndrome

Tomoko Fuke[1,2], Seiji Mizuno[3], Toshiro Nagai[4], Tomonobu Hasegawa[2], Reiko Horikawa[5], Yoko Miyoshi[6], Koji Muroya[7], Tatsuro Kondoh[8], Chikahiko Numakura[9], Seiji Sato[10], Kazuhiko Nakabayashi[11], Chiharu Tayama[11], Kenichiro Hata[11], Shinichiro Sano[1,12], Keiko Matsubara[1], Masayo Kagami[1], Kazuki Yamazawa[1], Tsutomu Ogata[1,12]*

1 Department of Molecular Endocrinology, National Research Institute for Child Health and Development, Tokyo, Japan, **2** Department of Pediatrics, Keio University School of Medicine, Tokyo, Japan, **3** Department of Pediatrics, Central Hospital, Aichi Human Service Center, Aichi, Japan, **4** Department of Pediatrics, Dokkyo Medical University Koshigaya Hospital, Saitama, Japan, **5** Division of Endocrinology and Metabolism, National Center for Child Health and Development, Tokyo, Japan, **6** Department of Pediatrics, Osaka University Graduate School of Medicine, Suita, Japan, **7** Department of Endocrinology and Metabolism, Kanagawa Children's Medical Center, Kanagawa, Japan, **8** Division of Developmental Disability, Misakaenosono Mutsumi Developmental, Medical, and Welfare Center, Isahaya, Japan, **9** Department of Pediatrics, Yamagata University School of Medicine, Yamagata, Japan, **10** Department of Pediatrics, Saitama Municipal Hospital, Saitama, Japan, **11** Department of Maternal-Fetal Biology, National Research Institute for Child Health and Development, Tokyo, Japan, **12** Department of Pediatrics, Hamamatsu University School of Medicine, Hamamatsu, Japan

Abstract

Background: Recent studies have revealed relative frequency and characteristic phenotype of two major causative factors for Silver-Russell syndrome (SRS), i.e. epimutation of the *H19*-differentially methylated region (DMR) and uniparental maternal disomy 7 (upd(7)mat), as well as multilocus methylation abnormalities and positive correlation between methylation index and body and placental sizes in *H19*-DMR epimutation. Furthermore, rare genomic alterations have been found in a few of patients with idiopathic SRS. Here, we performed molecular and clinical findings in 138 Japanese SRS patients, and examined these matters.

Methodology/Principal Findings: We identified *H19*-DMR epimutation in cases 1–43 (group 1), upd(7)mat in cases 44–52 (group 2), and neither *H19*-DMR epimutation nor upd(7)mat in cases 53–138 (group 3). Multilocus analysis revealed hyper- or hypomethylated DMRs in 2.4% of examined DMRs in group 1; in particular, an extremely hypomethylated *ARHI*-DMR was identified in case 13. Oligonucleotide array comparative genomic hybridization identified a ~3.86 Mb deletion at chromosome 17q24 in case 73. Epigenotype-phenotype analysis revealed that group 1 had more reduced birth length and weight, more preserved birth occipitofrontal circumference (OFC), more frequent body asymmetry and brachydactyly, and less frequent speech delay than group 2. The degree of placental hypoplasia was similar between the two groups. In group 1, the methylation index for the *H19*-DMR was positively correlated with birth length and weight, present height and weight, and placental weight, but with neither birth nor present OFC.

Conclusions/Significance: The results are grossly consistent with the previously reported data, although the frequency of epimutations is lower in the Japanese SRS patients than in the Western European SRS patients. Furthermore, the results provide useful information regarding placental hypoplasia in SRS, clinical phenotypes of the hypomethylated *ARHI*-DMR, and underlying causative factors for idiopathic SRS.

Citation: Fuke T, Mizuno S, Nagai T, Hasegawa T, Horikawa R, et al. (2013) Molecular and Clinical Studies in 138 Japanese Patients with Silver-Russell Syndrome. PLoS ONE 8(3): e60105. doi:10.1371/journal.pone.0060105

Editor: Monica Miozzo, Università degli Studi di Milano, Italy

Received September 7, 2012; **Accepted** February 21, 2013; **Published** March 22, 2013

Funding: This work was funded by Grants-in-Aid for Scientific Research (A) (22249010) and Research (B) (21028026) from the Japan Society for the Promotion of Science (http://www.jsps.go.jp/english/index.html), by Grant for Research on Rare and Intractable Diseases (H24-042) from the Ministry of Health, Labor and Welfare (http://www.mhlw.go.jp/english/), and by Grant for National Center for Child Health and Development (23A-1) (http://www.ncchd.go.jp/English/Englishtop.htm). The funders had no role in study design, data collection and analysis, decision to publish, or preparation of the manuscript.

Competing Interests: The authors have declared that no competing interests exist.

* E-mail: tomogata@hama-med.ac.jp

Introduction

Silver-Russell syndrome (SRS) is a rare congenital developmental disorder characterized by pre- and postnatal growth failure, relative macrocephaly, triangular face, hemihypotrophy, and fifth-finger clinodactyly [1]. Recent studies have shown that epimutation (hypomethylation) of the paternally derived differentially methylated region (DMR) in the upstream of *H19* (*H19*-DMR) on chromosome 11p15.5 and maternal uniparental disomy for chromosome 7 (upd(7)mat) account for ~45% and 5−10% of SRS patients, respectively [1,2]. In this regard, phenotypic assessment has suggested that birth length and weight are more reduced and characteristic body features are more frequent in patients with *H19*-DMR epimutation than in those with upd(7)mat, whereas developmental delay tends to be more

frequent in patients with upd(7)mat than in those with *H19*-DMR epimutation [3,4]. Furthermore, consistent with the notion that imprinted genes play an essential role in placental growth and development [5], placental hypoplasia has been found in both *H19*-DMR epimutation and upd(7)mat [4,6], although comparison of placental weight has not been performed between *H19*-DMR hypomethylation and upd(7)mat. In addition, multilocus hypo- or hypermethylation and positive correlation between methylation index (MI, the ratio of methylated clones) and body and placental sizes have been reported in patients with *H19*-DMR epimutation [4,7–9], and several types of rare genomic alterations have been identified in a few of SRS patients [1,10–12].

Here, we report on molecular and clinical findings in 138 Japanese SRS patients, and discuss on the results obtained in this study.

Patients and Methods

Ethics statement

This study was approved by the Institutional Review Board Committee at the National Center for Child Health and Development. The parents of the affected children and the adult patients who can express an intention by themselves have given written informed consent to participate in this study and to publish their molecular and clinical data.

Patients

This study consisted of 138 Japanese patients (66 males and 72 females) with SRS phenotype aged 0–30 years (median 4.1 years), including 64 previously reported patients (20 patients with variable degrees of *H19*-DMR epimutation, three patients with upd(7)mat, one patient with 46,XY/46,XY,upd(7)mat mosaicism in whom upd(7)mat cells accounted for 91–92% of leukocytes and salivary cells and for 11% of placental tissue, and 40 patients of unknown cause) [4,6,13]. The 138 patients had a normal karyotype in all the ≥50 lymphocytes examined, and satisfied the selection criteria proposed by Netchine et al. [14], i.e., birth length and/or birth weight ≤ −2 standard deviation score (SDS) for gestational age as a mandatory criteria plus at least three of the following five features: (i) postnatal short stature (≤ −2 SDS) at 2 year of age or at the nearest measure available, (ii) relative macrocephaly at birth, i.e., SDS for birth length or birth weight minus SDS for birth occipitofrontal circumference (OFC) ≤ −1.5, (iii) prominent forehead during early childhood, (iv) body asymmetry, and (v) feeding difficulties during early childhood. Birth and present length/height, weight, and OFC were assessed by the gestational/postnatal age- and sex-matched Japanese reference data from the Ministry of Health, Labor, and Welfare and the Ministry of Education, Science, Sports and Culture. Placental weight was assessed by the gestational age-matched Japanese reference data [15]. Clinical features were evaluated by clinicians at different hospitals who participated in this study, using the same clinical datasheet. The SRS patients were classified into three groups by the molecular studies, i.e., those with *H19*-DMR hypomethylation (epimutation) (group 1), those with upd(7)mat (group 2), and the remaining patients (group 3).

Primers and samples

Primers utilized in this study are shown in Table S1. Leukocyte genomic DNA samples were examined in this study.

Methylation analysis

We performed pyrosequencing analysis for the *H19*-DMR encompassing the 6th CTCF (CCCTC-binding factor) binding site that functions as the primary regulator for the monoallelic *IGF2* and *H19* expressions [16–18], using bisulfite treated leukocyte genomic DNA samples of all the 138 patients. The procedure was as described in the manufacturer's instructions (Qiagen, Valencia, CA, USA). In brief, a 279 bp region was PCR-amplified with a primer set (PyF and PyR) for both methylated and unmethylated clones, and a sequence primer (SP) was hybridized to a single-stranded PCR products. Subsequently, the MIs were obtained for four CpG dinucleotides (CG5–CG7 and CG9), using PyroMark Q24 (Qiagen) (the MI for CG8 was not obtained, because the "C" residue of CG8 constitutes a C/T SNP) (Figure 1A). The PyF/PyR and SP were designed by PyroMark Assay Design Software Ver2.0. While the PyF sequence contains a SNP (*rs11564736*) with a mean minor allele frequency of 5% in multiple populations, the minor allele frequency is 0% in the Japanese as well as in the Asian populations (http://browser.1000genomes.org/Homo_sapiens/Variation/Population?db=core;r=11:2020801–2021801;v=rs11564736;vdb=variation;vf=7864021). Thus, we utilized this PyF.

We also carried out combined bisulfite restriction analysis (COBRA) for the *H19*-DMR. The methods were as described previously [4]. In short, a 435 bp region was PCR-amplified with a primer set (CoF and CoR) that hybridize to both methylated and unmethylated clones, and MIs were obtained for two CpG dinucleotides (CG5 and CG16) after digestion of the PCR products with methylated allele-specific restriction enzymes (*Hpy*188I and *Afl*III) (Figure 1A).

Thus, we could examine CG5 by both pyrosequencing and COBRA. While we also attempted to analyze CG16 by both methods, it was impossible to design an SP for the analysis of CG16 (although we could design an SP between CG11 and CG12, clear methylation data were not obtained for CG16, probably because of the distance between the SP and CG16).

In addition, we performed COBRA for the KvDMR1 in all the 138 patients (Figure S1A) because of the possibility that epimutation of the KvDMR1 could lead to SRS phenotype via some mechanism(s) such as overexpression of a negative growth regulator *CDKN1C* [19], and for multiple DMRs on various chromosomes in patients in whom relatively large amount of DNA samples were available, as reported previously [4,20,21]. To define the reference ranges of MIs (minimum ~ maximum), 50 control subjects were similarly studied with permission.

To screen upd(7)mat, PCR amplification was performed for the *MEST*-DMR on chromosome 7q32.2 in all the 138 patients, using methylated and unmethylated allele-specific PCR primer sets, as reported previously [6] (Figure 2A). In addition, bisulfite sequencing and direct sequencing for the primer binding sites for the *ARHI*-DMR analysis were performed in a patient (case 13) with an extremely low MI for the *ARHI*-DMR.

Microsatellite analysis

Microsatellite analysis was performed for four loci within a ~4.5 Mb telomeric 11p region (*D11S2071*, *D11S922*, *D11S1318*, and *D11S988*) in patients with hypomethylated *H19*-DMR, to examine the possibility of upd(11p)mat involving the *H19*-DMR. Microsatellite analysis was also carried out for nine loci widely dispersed on chromosome 7 (Table S2) in patients with abnormal methylation patterns of the *MEST*-DMR, to examine the possibility of upd(7)mat and to infer the underlying causes for upd(7)mat, i.e., trisomy rescue, gamete complementation, monosomy rescue, and post-fertilization mitotic error [22]. The methods have been reported previously [4,6].

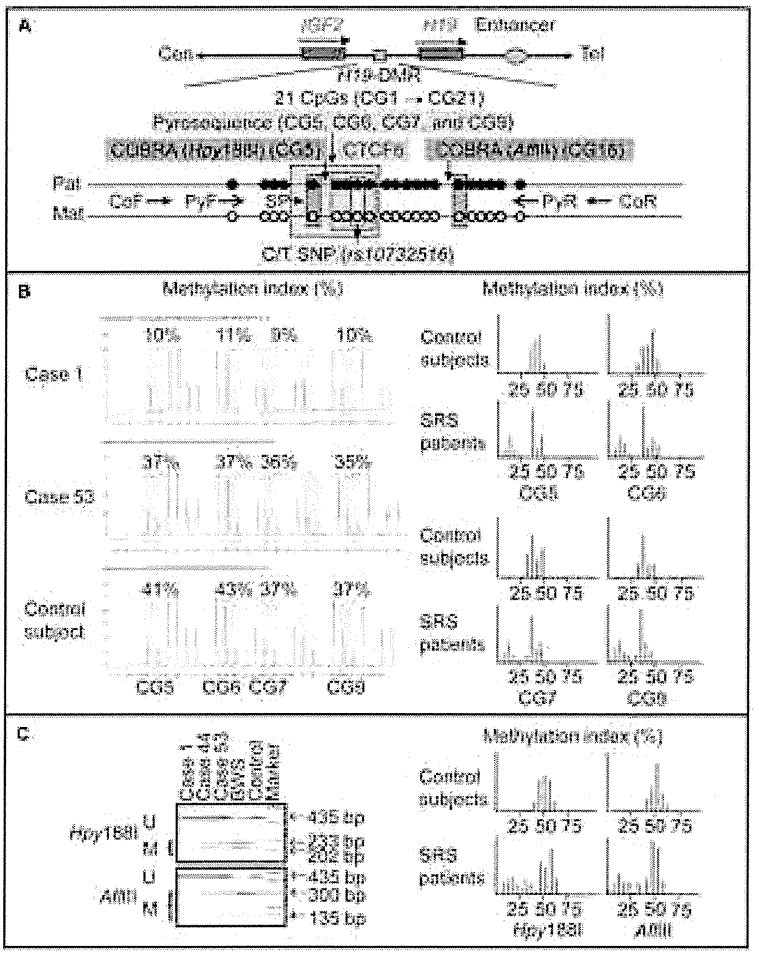

Figure 1. Methylation analysis of the *H19*-DMR, using bisulfite-treated genomic DNA. A. Schematic representation of a segment encompassing 21 CpG dinucleotides (CG1→CG21) within the *H19*-DMR. The cytosine residues at the CpG dinucleotides are usually methylated after paternal transmission (filled circles) and unmethylated after maternal transmission (open circles). The CTCF binding site 6 (CTCF6) is indicated with a blue rectangle; the cytosine residue at CG8 constitutes a C/T SNP (indicated with a gray rectangle). For pyrosequencing analysis, a 279 bp segment was PCR-amplified with PyF & PyR primers, and a sequence primer (SP) was hybridized to a single-stranded PCR products. Subsequently, the MIs were obtained for four CpG dinucleotides (CG5–CG7 and CG9) (indicated with a yellow rectangle). For COBRA, a 435 bp region was PCR-amplified with CoF & CoR primers, and the PCR product was digested with methylated allele-specific restriction enzymes to examine the methylation pattern of CG5 ands CG16 (the PCR products is digested with *Hpy*188I when the cytosine residue at CG5 is methylated and with *Afl*III when the cytosine residue at CG16 is methylated) (indicated with orange rectangles). *IGF2* is a paternally expressed gene, and *H19* is a maternally expressed gene. The stippled ellipse indicates the enhancer for *IGF2* and *H19*. B. Pyrosequencing data. Left part: Representative results indicating the MIs for CG5– CG7 and CG9. CG5– CG7 and CG9 are hypomethylated in case 1, and similarly methylated between case 53 and a control subject. Right part: Histograms showing the distribution of the MIs (the horizontal axis: the methylation index; and the vertical axis: the patient number). Forty-three SRS patients with low MIs are shown in red. C. COBRA data. Left part: Representative findings of PCR products loaded onto a DNA 1000 LabChip (Agilent, Santa Clara, CA, USA) after digestion with *Hpy*188I or *Afl*III. U: unmethylated clone specific bands; M: methylated clone specific bands; and BWS: Beckwith-Wiedemann syndrome patient with upd(11p15)pat. Right part: Histograms showing the distribution of the MIs.
doi:10.1371/journal.pone.0060105.g001

Oligoarray comparative genomic hybridization (CGH)

We performed oligoarray CGH in the 138 SRS patients, using a genomewide 4×180K Agilent platform catalog array and a custom-build high density oligoarray for the 11p15.5, 7p12.2, 12q14, and 17q24 regions where rare copy number variants have been identified in several SRS patients [1,10–12] as well as for the 7q32–qter region involved in the segmental upd(7)mat in four SRS patients [23–25]. The custom-build high density oligoarray contained 3,214 probes for 7p12.2, 434 probes for 7q32, 23,162 probes for 12q14, and 39,518 probes for 17q24, together with ~10,000 reference probes for other chromosomal region (Agilent Technologies, Palo Alto, CA, USA). The procedure was as described in the manufacturer's instructions.

Statistical analysis

After examining normality by χ^2 test, the variables following the normal distribution were expressed as the mean±SD, and those not following the normal distribution were expressed with the

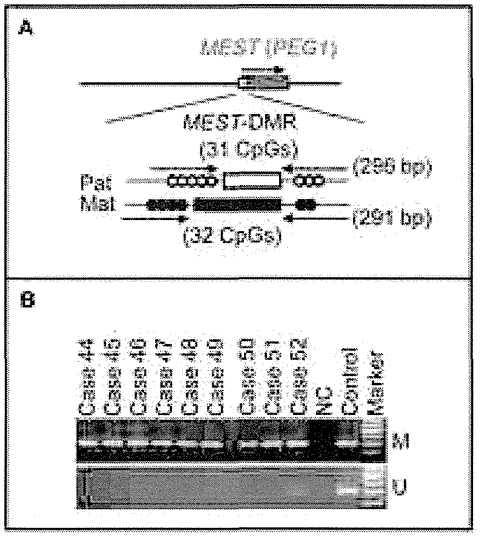

Figure 2. Methylated and unmethylated allele-specific PCR analysis for the *MEST*-DMR. A. Schematic representation of the *MEST*-DMR. The cytosine residues at the CpG dinucleotides are usually unmethylated after paternal transmission (open circles) and methylated after maternal transmission (filled circles). The PCR primers have been designed to hybridize either methylated or unmethylated clones. B. The results of methylation analysis with methylated and unmethylated allele-specific primers.
doi:10.1371/journal.pone.0060105.g002

median and range. Statistical significance of the mean was analyzed by Student's *t*-test or Welch's *t*-test after comparing the variances by *F* test, that of the median by Mann-Whitney's *U*-test, that of the frequency by Fisher's exact probability test, and that of the correlation by Pearson's correlation coefficient after confirming the normality of the variables. $P<0.05$ was considered significant.

Results

Identification of *H19*-DMR hypomethylation

Representative findings are shown in Figure 1B and 1C, and the MIs are summarized in Table 1. Overall, the MIs obtained by the pyrosequencing analysis tended to be lower and distributed more narrowly than those obtained by the COBRA. Despite such difference, the MIs obtained by the pyrosequencing analysis for CG5–CG7 and CG9 and by the COBRA for CG5 and CG16 were invariably below the normal range in the same 43 patients (cases 1–43) (group 1). By contrast, the MIs were almost invariably within the normal range in the remaining 95 patients, while the MIs obtained by the pyrosequencing analysis slightly (1–2%) exceeded the normal range in the same three patients (cases 136–138).

In the 43 cases of group 1, microsatellite analysis for four loci at the telomeric 11p region excluded maternal upd in 14 cases in whom parental DNA samples were available; in the remaining 29 cases, microsatellite analysis identified two alleles for at least one locus, excluding maternal uniparental isodisomy for this region. Furthermore, oligoarray CGH for the chromosome 11p15.5 region showed no copy number alteration such as duplication of maternally derived *H19*-DMR and deletion of paternally derived *H19*-DMR. For the KvDMR1, the MIs of the 138 patients remained within the reference range (Fig. S1B and C).

Table 1. The methylation indices (%) for the *H19*-DMR.

	Cases 1–43	Cases 44–138	Control subjects
Pyrosequencing analysis			
CG5	4–24	35–50	33–48
CG6	5–26	36–53	34–51
CG7	4–24	35–49	30–47
CG9	5–23	34–48	30–46
COBRA			
CG5 (*Hpy*188I)	3.3–35.1	37.8–60.8	36.2–58.5
CG16 (*Afl*III)	4.1–35.0	43.0–59.4	38.7–60.0

The position of examined CpG dinucleotides (CG5–7, CG9, and CG16) is shown in Figure 1A.
COBRA: combined bisulfite restriction analysis.
doi:10.1371/journal.pone.0060105.t001

Identification of upd(7)mat

Methylation analysis for the *MEST*-DMR revealed that unmethylated bands were absent from eight patients and remained faint in a single patient (cases 44–52) (group 2) (Figure 2B). Subsequent microsatellite analysis confirmed upd(7)mat in the eight patients and mosaic upd(7)mat in the remaining one patient, and indicated trisomy rescue or gamete complementation type upd(7)mat in cases 44–48, monosomy rescue or post-fertilization mitotic error type upd(7)mat in cases 49–51, and post-fertilization mitotic error type mosaic upd(7)mat in case 52 (Table S2).

Multiple DMR analysis

We examined 17 autosomal DMRs other than the *H19*-DMR in 14 patients in group 1, four patients in group 2, and 20 patients in group 3, and the *XIST*-DMR in eight female patients in group 1, one female patient in group 2, and five female patients in group 3 (Table S3). The MIs outside the reference ranges were identified in five of 14 examined cases (35.7%) and six of a total of 246 examined DMRs (2.4%) in group 1. In particular, a single case with the mean MI value of 23 obtained by the pyrosequencing analysis for CG5–CG7 and CG9 had an extremely low MI for the *ARHI*-DMR (case 13 of group 1). This extreme hypomethylation was confirmed by bisulfite sequencing, and direct sequencing showed normal sequences of the primer-binding sites, thereby excluding the possibility that such an extremely low MI could be due to insufficient primer hybridization because of the presence of a nucleotide variation within the primer-binding sites (Figure 3). Furthermore, no copy number variation involving the *ARHI*-DMR was identified by CGH analysis using a genomewide catalog array. Consistent with upd(7)mat, three DMRs on chromosome 7 were extremely hypermethylated in four examined cases of group 2. Only a single DMR was mildly hypermethylated in a total of 345 examined DMRs in group 3. The abnormal MIs, except for those for the *H19*-DMR in group 1 and for the three DMRs on chromosome 7 in group 2, were confirmed by three times experiments.

Oligonucleotide array CGH

A ~3.86 Mb deletion at chromosome 17q24 was identified in a single patient (case 73 of group 3) (Figure 4).

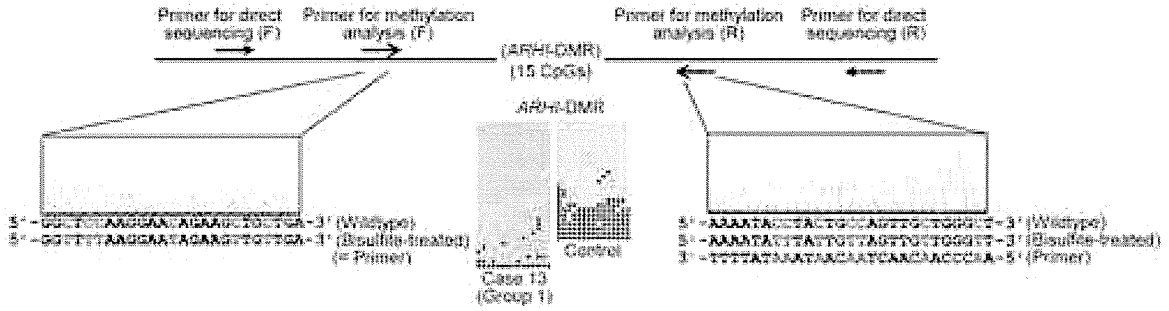

Figure 3. Analysis of the *ARHI*-DMR in case 13. For bisulfite sequencing, each line indicates a single clone, and each circle denotes a CpG dinucleotide; the cytosine residues at the CpG dinucleotides are usually unmethylated after paternal transmission (open circles) and methylated after maternal transmission (filled circles). Electrochromatograms delineate the sequences of the primer binding sites utilized for the methylation analysis.
doi:10.1371/journal.pone.0060105.g003

Epigenotype-phenotype analysis

Clinical findings of SRS patients in groups 1–3 are summarized in Table 2. All the patients met the mandatory criteria, and most patients in each group had severely reduced birth length and weight (both≤−2 SDS). For the five clinical features utilized as scoring system criteria, while 23.2% of patients in group 1 and 22.2% of patients in group 2 exhibited all the five features, there was no patient in group 3 who was positive for all the five features. By contrast, while 39.5% of patients in group 1 and 33.3% of patients in group 2 manifested just three of the five features, 77.6% of patients in group 3 were positive for just three features. In particular, the frequencies of relative macrocephaly at birth and body asymmetry were low in group 3, while those of the remaining three scoring system criteria including prominent forehead during early childhood were similar among groups 1–3.

Phenotypic comparison between groups 1 and 2 revealed that birth length and weight were more reduced and birth OFC was more preserved in group 1 than in group 2, despite comparable gestational age. In the postnatal life, present height and weight became similar between the two groups, whereas present OFC became significantly smaller in group 1 than in group 2. Body asymmetry and brachydactyly were more frequent and speech delay was less frequent in group 1 than in group 2. Placental weight was similar between the two groups, and became more similar after excluding case 52 with mosaic upd(7)mat (see legends for Table 2). Parental age at childbirth was also similar between the two groups. In group 2, placental weight was grossly similar among examined cases, as was parental age at childbirth (see legends for Table 2).

Case 13 with an extremely low MI for the *ARHI*-DMR and case 73 with a cryptic deletion at chromosome 17q24 had no specific phenotype other than SRS-like phenotype (Table S4). However, of the five clinical features utilized as scoring system criteria, all the five features were exhibited by case 13 and just three features were

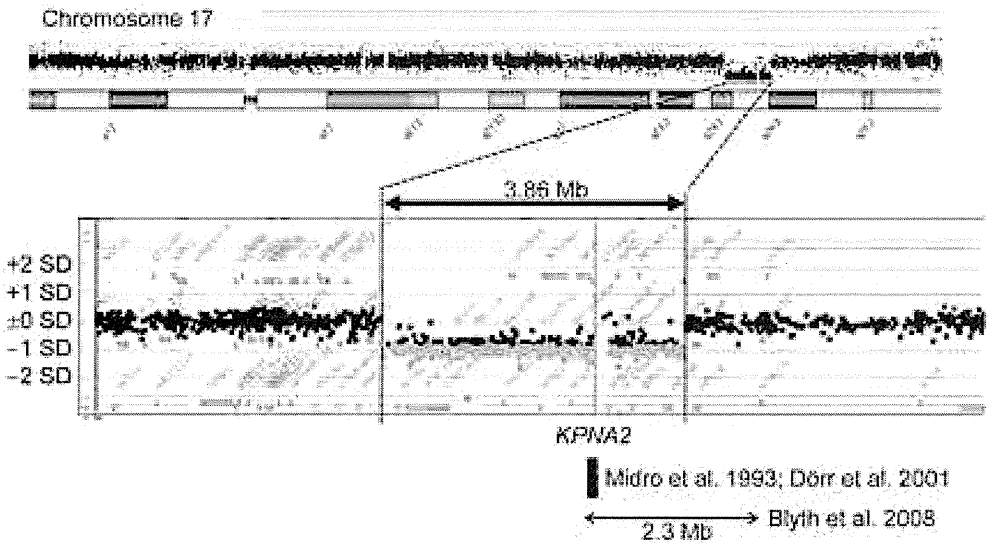

Figure 4. Oligonucleotide array CGH in case 73, showing a ~3.86 Mb deletion at chromosome 17q24. The black, the red, and the green dots denote signals indicative of the normal, the increased(>+0.5), and the decreased (< −1.0) copy numbers, respectively. The horizontal bar with arrowheads indicates a ~2.3 Mb deletion identified in a patient with Carney complex and SRS-like phenotype [44], and the black square represent a ~65 kb segment harboring the breakpoint of a *de novo* translocation 46,XY,t(1;17)(q24;q23–q24) identified in a patient with SRS phenotype [45,46].
doi:10.1371/journal.pone.0060105.g004

Table 2. Phenotypic comparison in three groups of patients with Silver-Russell syndrome.

	H19-DMR hypomethylation	Upd(7)mat	Unknown	*P*-value		
	(Group 1)	(Group 2)	(Group 3)	G1 vs. G2	G1 vs. G3	G2 vs. G3
Patient number	43 (31.2%)	9 (6.5%)	85 (62.0%)			
Mandatory criteria	43/43 (100%)	9/9 (100%)	85/85 (100%)	1.000	1.000	1.000
Scoring system criteria (5/5)	10/43 (23.2%)	2/9 (22.2%)	0/85 (0.00%)	0.965	**1.52×10^{-4}**	**2.58×10^{-2}**
Scoring system criteria (4/5)	16/43 (37.2%)	4/9 (44.4%)	19/85 (22.4%)	0.792	**1.45×10^{-2}**	0.145
Scoring system criteria (3/5)	17/43 (39.5%)	3/9 (33.3%)	66/85 (77.6%)	0.821	**7.17×10^{-4}**	0.161
Gestational age (weeks:days)	38:0 (34:3~40:0) (n = 36)	38:0 (34:4~40:0) (n = 9)	37:6 (27:1~41:4) (n = 65)	0.877	0.120	0.450
BL (SDS)	−4.13±2.01 (n = 31)	−3.18±1.16 (n = 9)	−2.93±1.43 (n = 60)	**2.67×10^{-2}**	**6.69×10^{-5}**	0.619
BW (SDS)	−3.50±0.85 (n = 42)	−2.90±0.64 (n = 9)	−2.71±1.14 (n = 64)	**3.28×10^{-2}**	**5.87×10^{-4}**	0.640
BL≤−2 SDS and/or BW≤−2 SDS*	43/43 (100%)	9/9 (100%)	85/85 (100%)	1.000	1.000	1.000
BL≤−2 SDS and BW≤−2 SDS	39/43 (90.7%)	7/9 (77.8%)	76/85 (89.4%)	0.474	0.821	0.304
BOFC (SDS)	−0.54±1.22 (n = 29)	−1.44±0.47 (n = 9)	−1.92±1.09 (n = 48)	**3.74×10^{-2}**	**1.52×10^{-6}**	0.202
BL (SDS) − BOFC (SDS)	−3.70±2.02 (n = 27)	−1.73±1.20 (n = 9)	−0.943±1.48 (n = 43)	**1.02×10^{-2}**	**3.40×10^{-9}**	0.111
BW (SDS) − BOFC (SDS)	−3.21±1.20 (n = 27)	−1.53±0.57 (n = 9)	−1.04±1.55 (n = 48)	0.326	**7.38×10^{-9}**	0.331
Relative macrocephaly at birth† BL or BW (SDS) − BOFC (SDS)≤−1.5	29/29 (100%)	7/9 (77.8%)	16/45 (35.6%)	0.341	**3.67×10^{-8}**	**2.05×10^{-2}**
Present age (years:months)	4.1 (0:6~30:6) (n = 31)	4.8 (2:4~25:2) (n = 9)	4.3 (0:1~18:6) (n = 60)	0.437	0.813	0.335
PH (SDS)	−3.58±1.65 (n = 35)	−3.77±1.13 (n = 9)	−3.17±1.50 (n = 61)	0.757	0.218	0.253
PH≤−2 SDS (≥2 years)†	29/35 (82.5%)	8/9 (88.9%)	52/61 (85.2%)	0.760	0.758	0.772
PW (SDS)	−3.15±1.16 (n = 32)	−2.77±0.76 (n = 9)	−2.77±1.34 (n = 59)	0.362	0.144	0.968
POFC (SDS)	−1.16±1.18 (n = 21)	−0.01±0.91 (n = 9)	−1.81±1.57 (n = 35)	**2.01×10^{-3}**	0.107	**3.08×10^{-3}**
PH (SDS) − POFC (SDS)	−2.47±1.63 (n = 16)	−3.62±1.38 (n = 8)	−1.55±1.82 (n = 35)	0.103	**4.39×10^{-2}**	**1.64×10^{-2}**
PW (SDS) − POFC (SDS)	−2.84±1.31 (n = 21)	−2.69±1.36 (n = 9)	−1.08±1.71 (n = 35)	0.782	**2.54×10^{-2}**	**1.90×10^{-4}**
Relative macrocephaly at present PH or PW (SDS) − POFC (SDS)≤−1.5	20/21 (95.2%)	8/8 (100%)	29/43 (67.4%)	0.223	**4.77×10^{-3}**	0.156
Triangular face during early childhood	42/43 (97.7%)	8/9 (88.9%)	65/65 (100%)	0.442	0.0773	**5.98×10^{-3}**
Prominent forehead during early childhood†	31/37 (83.8%)	7/9 (100%)	41/53 (77.4%)	0.200	0.456	0.978
Ear anomalies	14/35 (40.0%)	3/9 (33.3%)	15/55 (27.3%)	0.717	0.290	0.823
Irregular teeth	12/26 (46.2%)	4/9 (44.4%)	12/45 (26.7%)	0.930	0.0968	0.291
Body asymmetry†	30/37 (81.1%)	3/9 (33.3%)	19/59 (32.2%)	**4.77×10^{-3}**	**3.51×10^{-6}**	0.947
Clinodactyly	29/37 (78.4%)	5/9 (55.6%)	50/58 (86.2%)	0.167	0.323	**2.68×10^{-2}**
Brachydactyly	30/38 (78.9%)	2/9 (22.2%)	34/56 (60.7%)	1.16×10^{-3}	0.0642	**3.24×10^{-2}**
Syndactyly	3/36 (8.3%)	0/9 (0.00%)	3/52 (5.77%)	0.375	0.641	0.464
Simian crease	4/26 (15.4%)	2/7 (28.6%)	6/49 (12.2%)	0.429	0.705	0.252
Muscular hypotonia	17/32 (53.1%)	5/9 (55.6%)	12/50 (24.0%)	0.898	**7.49×10^{-3}**	0.0564
Developmental delay	18/37 (48.6%)	6/9 (66.7%)	25/54 (46.3%)	0.337	0.826	0.262
Speech delay	8/31 (25.8%)	6/9 (66.7%)	18/43 (41.9%)	**2.55×10^{-2}**	0.156	0.179
Feeding difficulty†	16/34 (47.1%)	6/9 (66.7%)	25/51 (49.0%)	0.301	0.860	0.333
Placental weight (SDS)	−2.10±0.74 (n = 14)	−1.72 ± 0.74 (n = 6)[a]	−1.02±0.86 (n = 18)	0.312	**4.12×10^{-3}**	**8.24×10^{-3}**
Paternal age at childbirth (years:months)	32:0 (19:0~52:0) (n = 24)	35:0 (27:0~48:0) (n = 9)	32:0 (25:0~46:0) (n = 45)	0.223	1.00	0.105
Maternal age at childbirth (years:months)	32:0 (19:0~43:0) (n = 25)	33:0 (25:0~42:0) (n = 9)[b]	30:0 (22:0~43:0) (n = 46)	0.275	0.765	0.117

BL: birth length; BW: birth weight; BOFC: birth occipitofrontal circumference; PH: present height; PW: present weight; POFC: present occipitofrontal circumference, and SDS: standard deviation score.

For body features, the denominators indicate the number of patients examined for the presence or absence of each feature, and the numerators represent the number of patients assessed to be positive for that feature.

*Mandatory criteria and †five clinical features utilized as selection criteria for Silver-Russell syndrome proposed by Netchine et al. [14].

Significant *P*-values(<0.05) are boldfaced.

[a]Placental weight SDS is −1.68, −2.55, −2.24, −1.12, −2.14 and −0.60 in case 46, 47, 49, 50, 51 and 52, respectively; the placental weight SDS is −1.95±0.57 in five cases except for case 52 with mosaic upd(7)mat.

[b]Maternal childbearing age is 32, 32, 33, 42, 32, 34, 33, 25 and 36 years in case 44–52, respectively.

doi:10.1371/journal.pone.0060105.t002

manifested by case 73. In addition, cases 136–138 with slightly elevated MIs for CG5–CG7 and CG9, and cases with multilocus methylation abnormalities, had no particular phenotype other than SRS-compatible clinical features.

Correlation analysis

In group 1, the mean value of the MIs for CG5–CG7 and CG9 obtained by pyrosequencing analysis was positively correlated with the birth length and weight, the present height and weight, and the placental weight, but with neither the birth nor the present OFC (Table 3). Such correlations with the growth parameters were grossly similar but somewhat different for the MIs obtained by COBRA (Table S5). Furthermore, the placental weight was positively correlated with the birth weight and length, but not with the birth OFC. Such positive correlations were not found in groups 2 and 3.

Discussion

The present study identified hypomethylation of the *H19*-DMR and upd(7)mat in 31.2% and 6.5% of 138 Japanese SRS patients, respectively. In this regard, the normal KvDMR1 methylation patterns indicate that the aberrant methylation in 43 cases of group 1 is confined to the *H19*-DMR. Furthermore, oligoarray CGH excludes copy number variants involving the *H19*-DMR, and microsatellite analysis argues against segmental maternal isodisomy that could be produced by post-fertilization mitotic error [26]. These findings imply that the *H19*-DMR hypomethylation is due to epimutation (hypomethylation of the normally methylated *H19*-DMR of paternal origin).

The frequency of epimutations detected in this study is lower than that reported in Western European SRS patients [1,2,14], although the frequency of upd(7)mat is grossly similar between the two populations [2,11,14,27,28]. In this context, it is noteworthy that, of the five scoring system criteria, the frequencies of relative macrocephaly at birth and body asymmetry were low in group 3, while those of the remaining three scoring system criteria were similar among groups 1–3. Since relative macrocephaly and body asymmetry are characteristic of *H19*-DMR epimutation, the lack of these two features in a substantial fraction of cases in group 3 would primarily explain the low frequency of *H19*-DMR epimutations in this study. In group 3, furthermore, the low prevalence of relative macrocephaly at birth appears to be discordant with the high prevalence of prominent forehead during early childhood. Since relative macrocephaly was evaluated by an objective method (SDS for birth length or birth weight minus SDS for birth OFC≤−1.5) and prominent forehead was assessed by a subjective impression of different clinicians, it is recommended to utilize relative macrocephaly as a more important and reliable feature in the scoring system than prominent forehead. In addition, the difference in the ethnic group might also be relevant to the low frequency of *H19*-DMR epimutations in this study.

Table 3. Correlation analyses in patients with *H19*-DMR hypomethylations.

Parameter 1	Parameter 2	*r*	*P*-value
Methylation index (%)* vs.	Birth length (SDS)	0.647	**6.70×10^{-3}**
	Birth weight (SDS)	0.590	**7.80×10^{-3}**
	Birth OFC (SDS)	0.190	0.498
	Present height (SDS)	0.612	**5.33×10^{-3}**
	Present weight (SDS)	0.605	**7.81×10^{-3}**
	Present OFC (SDS)	−0.166	0.647
	Placental weight (SDS)	0.809	**8.30×10^{-3}**
Placental weight (SDS) vs.	Birth weight (SDS)	0.717	**8.64×10^{-3}**
	Birth length (SDS)	0.636	**2.63×10^{-2}**
	Birth OFC (SDS)	0.400	0.198

SDS: standard deviation score; and OFC: occipitofrontal circumference.
*The mean value of MIs for CG5, CG6, CG7, and CG9 obtained by pyrosequencing analysis.
Significant *P*-values(<0.05) are boldfaced.
doi:10.1371/journal.pone.0060105.t003

Epigenotype-phenotype correlations in this study are grossly similar to those previously reported in Western European SRS patients [1–3]. Cases 1–43 in group 1 with *H19*-DMR epimutation had more reduced birth weight and length, more preserved birth OFC and more reduced present OFC, more frequent body features, and less frequent speech delay than case 44–52 in group 2 with upd(7)mat, although the difference in the prevalence of somatic features appears to be less remarkable in this study than in the previous studies [3,4]. This provides further support for the presence of relatively characteristic clinical features in *H19*-DMR epimutation and upd(7)mat [1–3]. In this context, previous studies have indicated biallelic *IGF2* expression in the human fetal choroid plexus, cerebellum, and brain, and monoallelic *IGF2* expression in the adult brain, while the precise brain tissue(s) with such a unique expression pattern remains to be clarified [29,30,31]. This may explain why the birth OFC is well preserved and the present OFC is reduced in group 1. However, since the difference in present OFC between groups 1 and 2 is not necessarily significant in the previous studies [32], the postnatal OFC growth awaits further investigations.

Placental weight was similarly reduced in groups 1 and 2. Thus, placental weight is unlikely to represent an indicator for the discrimination between the two groups, although the present data provide further support for imprinted genes being involved in placental growth, with growth-promoting effects of *PEGs* and growth-suppressing effects of *MEGs* [5,6]. It should be pointed out, however, that the placental hypoplasia could be due to some other genetic or environmental factor(s). In particular, while placental weight was apparently similar among cases of group 2, possible confined placental mosaicism [33,34] with trisomy for chromosome 7 may have exerted some effects on placental growth in cases with trisomy rescue type upd(7)mat.

Correlation analysis would imply that the *IGF2* expression level, as reflected by the MI of the *H19*-DMR, plays a critical role in the determination of pre- and postnatal body (stature and weight) and placental growth in patients with *H19*-DMR epimutation. Since the placental weight was positively correlated with the birth length and weight, the reduced *IGF2* expression level appears to have a similar effect on the body and the placental growth. Furthermore, the lack of correlations between the MI and birth and present OFC and between placental weight and birth OFC would be compatible with the above mentioned *IGF2* expression pattern in the central nervous system [29]. Although the MI would also reflect the *H19* expression level, this would not have a major growth effect. It has been implicated that *H19* functions as a tumor suppressor [35,36].

Multilocus analysis revealed co-existing hyper- and hypomethylated DMRs predominantly in cases of group 1, with frequencies of 35.7% of examined patients and 2.4% of examined DMRs. The results are grossly consistent with the previous data indicating that co-existing abnormal methylation patterns of DMRs are almost exclusively identified in patients with *H19*-DMR epimutation with frequencies of 9.5~30.0% of analyzed patients and 1.8~5.2% of a

total of analyzed DMRs [7–9]. Notably, the co-existing methylation abnormalities were predominantly observed as mild hypermethylations of maternally methylated DMRs and were restricted to a single DMR or two DMRs in patients with multilocus abnormalities. Such findings are obviously inexplicable not only by assuming a *ZFP57* mutation that is known to cause severely abnormal methylation patterns of multiple DMRs or a *ZAC1* mutation that may affect methylation patterns of multiple DMRs [37–39], but also by assuming defective maintenance of methylation in the postzygotic period [7]. Thus, some factor(s) susceptible to the co-occurrence of hypomethylation of the *H19*-DMR and hypermethylation of other DMR(s) might be operating during a gametogenic or postzygotic period in cases with *H19*-DMR epimutation.

The patients with multilocus methylation abnormalities had no specific clinical features other than SRS-compatible phenotype. Previous studies have also indicated grossly similar SRS-like phenotype between patients with monolocus and multilocus hypomethylations [7], although patients with multilocus hypomethylation occasionally have apparently severe clinical phenotype [7]. These findings would argue for the notion that the *H19*-DMR epimutation has an (epi)dominant clinical effect. Indeed, *H19*-DMR hypomethylation has led to SRS-like phenotype in a patient with parthenogenetic chimerism/mosaicism [21], whereas *H19*-DMR hypermethylation has resulted in Beckwith-Wiedemann syndrome-like phenotype in patients with androgenetic mosaicism [40].

An extremely hypomethylated *ARHI*-DMR was found in case 13. In this regard, it is known that *ARHI* with a potentially cell growth suppressor function is normally expressed from paternally inherited chromosome with unmethylated *ARHI*-DMR [41]. Indeed, hypermethylation of the *ARHI*-DMR, which is predicted to result in reduced expression of *ARHI*, has been identified as a tumorigenic factor for several cancers with an enhanced cell growth function [42,43]. Thus, it is possible that hypomethylation of the *ARHI*-DMR has led to overexpression of *ARHI*, contributing to the development of typical SRS phenotype in the presence of a low but relatively preserved MI of the *H19*-DMR in case 13.

Oligonucleotide array CGH identified a ~3.86 Mb deletion at chromosome 17q24 in case 73 of group 3. This provides further support for the presence of rare copy number variants in several SRS patients and the relevance of non-imprinted gene(s) to the development of SRS [10]. Interestingly, the microdeletion overlap with that identified in a patient with Carney complex and SRS-like features [44], and the overlapping region encompasses a ~65 kb segment defining the breakpoint of a *de novo* reciprocal translocation involving 17q23–q24 in a patient with SRS-like phenotype (Figure 4) [45,46]. Furthermore, the translocation breakage has affected *KPNA2* involved in the nuclear transport of proteins [46–48]. Thus, *KPNA2* has been regarded as a candidate gene for SRS, although mutation analysis of *KPNA2* has failed to detect a disease-causing mutation in SRS patients [49].

Lastly, it would be worth discussing on the comparison between pyrosequencing analysis and COBRA. Since the same 43 patients were found to have low MIs by both analyses, this implies that both methods can be utilized as a diagnostic tool. While the distribution of the MIs was somewhat different between the two methods, this would primarily be due to the difference in the employed methods such as the hybridization efficiency of utilized primers. Importantly, pyrosequencing analysis was capable of studying plural CpG dinucleotides at the CTCF6 binding site, whereas COBRA examined only single CpG dinucleotides outside the CTCF6 binding site. Thus, the MIs obtained by pyrosequencing analysis would be more accurate than those obtained by COBRA in terms of *IGF2* expression levels, and this would underlie the reasonable correlations of MIs yielded by pyrosequencing analysis with body and placental growth parameters.

In summary, the present study provides useful information for the definition of molecular and clinical findings in SRS. However, several matters still remain to be elucidated, including underlying mechanisms in SRS patients with no *H19*-DMR epimutation or upd(7)mat and the DMR(s) and imprinted gene(s) responsible for the development of SRS in patients with upd(7)mat. Furthermore, while advanced maternal age at childbirth has been shown to be a predisposing factor for the development of upd(15)mat because of increased non-disjunction at meiosis 1 [50], such studies remain fragmentary for upd(7)mat, primarily because of the relative paucity of upd(7)mat. Further studies will permit a better characterization of SRS.

Supporting Information

Figure S1 Methylation analysis of the KvDMR1 using COBRA. A. Schematic representation of the KvDMR1. A 326 bp region harboring 24 CpG dinucleotides was studied. The cytosine residues at the CpG dinucleotides are usually methylated after paternal transmission (filled circles) and unmethylated after maternal transmission (open circles); after bisulfite treatment, this region is digested with *Hpy*188I when the cytosine at the 5th CpG dinucleotide (indicated with a green rectangle) is methylated and with *Eci*I when the cytosines at the 22nd CpG dinucleotide (indicated with a pink rectangle) is methylated. *KCNQ1OT1* is a paternally expressed gene, and *KCNQ1* and *CDKN1C* are maternally expressed genes. B. Representative COBRA results. U: unmethylated clone specific bands; M: methylated clone specific bands; and BWS: Beckwith-Wiedemann syndrome patient with upd(11p15)pat. C. Histograms showing the distribution of the MIs (the horizontal axis: the methylation index; and the vertical axis: the patient number).
(TIF)

Table S1 Primers utilized in the methylation analysis and microsatellite analysis.
(XLS)

Table S2 The results of microsatellite analysis.
(XLSX)

Table S3 Methylation indices for multiple differetially methylated resions (DMRs) obtained by COBRA in 38 patients with Silver-Russell syndrome.
(XLSX)

Table S4 Clinical findings in two unique patients.
(DOC)

Table S5 Correlation analyses in patients with H19-DMR hypomethylations.
(DOC)

Acknowledgments

We would like to thank the following doctors for providing us with blood samples and clinical data: Toshio Yamazaki, Yukihiro Hasegawa, Daisuke Ariyasu, Michiko Hayashidani, Hiroshi Yoshihashi, Tomoki Kosho, Rika Kosaki, Yasuhiro Naiki, Hideki Fujita, Aya Yamashita, Katsuhiro Maeyama, Sayu Omori, Takashi Koike, Makoto Ono, Sachiko Kitanaka, Jun Mori, Shinichiro Miyagawa, Masamichi Ogawa, Toshiaki Tanaka, Naomi Hizuka, Yoko Fujimoto, Zenro Kizaki, Fumio Katsushima, Takashi Iwamoto, Wakako Yamamoto, Hotaka Kamasaki, Shun Soneda, Takahiro Tajima, Yoriko Watanabe, Kanako Ishii, Noriko Kinoshita, Tohjyu Tanaka, Eriko Nishi, Tohru Yorifuji, Yoshio Makita, Yoshinobu Honda, Junko Tsubaki, Yoko Shimabukuro, Yoko Hiraki, Kazushige

Dobashi, Kazumichi Onigata, Hisaaki Kabata, Shigeki Ishii, Kimiko Taniguchi, and Masaoki Sugita. We are also grateful to Drs. Kyoko Tanabe and Kentaro Matsuoka for their technical assistance.

Author Contributions

Conceived and designed the experiments: TF KY TO. Performed the experiments: TF KN CT S. Sano K. Matsubara MK KY. Analyzed the data: TF KN KH KY. Contributed reagents/materials/analysis tools: SM TN TH RH YM K. Muroya TK CN S. Sato TO. Wrote the paper: TO.

References

1. Eggermann T (2010) Russell-Silver syndrome. Am J Med Genet C Semin Med Genet 154C: 355–364.
2. Binder G, Begemann M, Eggermann T, Kannenberg K (2011) Silver-Russell syndrome. Best Pract Res Clin Endocrinol Metab 25: 153–160.
3. Wakeling EL, Amero SA, Alders M, Bliek J, Forsythe E, et al. (2010) Epigenotype-phenotype correlations in Silver-Russell syndrome. J Med Genet 47: 760–768.
4. Yamazawa K, Kagami M, Nagai T, Kondoh T, Onigata K, et al. (2008) Molecular and clinical findings and their correlations in Silver-Russell syndrome: implications for a positive role of IGF2 in growth determination and differential imprinting regulation of the IGF2-H19 domain in bodies and placentas. J Mol Med (Berl) 86: 1171–1181.
5. Fowden AL, Sibley C, Reik W, Constancia M (2006) Imprinted genes, placental development and fetal growth. Horm Res 65 Suppl 3: 50–58.
6. Yamazawa K, Kagami M, Ogawa M, Horikawa R, Ogata T (2008) Placental hypoplasia in maternal uniparental disomy for chromosome 7. Am J Med Genet A 146A: 514–516.
7. Azzi S, Rossignol S, Steunou V, Sas T, Thibaud N, et al. (2009) Multilocus methylation analysis in a large cohort of 11p15-related foetal growth disorders (Russell Silver and Beckwith Wiedemann syndromes) reveals simultaneous loss of methylation at paternal and maternal imprinted loci. Hum Mol Genet 18: 4724–4733.
8. Turner CL, Mackay DM, Callaway JL, Docherty LE, Poole RL, et al. (2010) Methylation analysis of 79 patients with growth restriction reveals novel patterns of methylation change at imprinted loci. Eur J Hum Genet 18: 648–655.
9. Hiura H, Okae H, Miyauchi N, Sato F, Sato A, et al. (2012) Characterization of DNA methylation errors in patients with imprinting disorders conceived by assisted reproduction technologies. Hum Reprod 27: 2541–2548.
10. Abu-Amero S, Monk D, Frost J, Preece M, Stanier P, et al. (2008) The genetic aetiology of Silver-Russell syndrome. J Med Genet 45: 193–199.
11. Hitchins MP, Stanier P, Preece MA, Moore GE (2001) Silver-Russell syndrome: a dissection of the genetic aetiology and candidate chromosomal regions. J Med Genet 38: 810–819.
12. Spengler S, Schönherr N, Binder G, Wollmann HA, Fricke-Otto S, et al. (2010) Submicroscopic chromosomal imbalances in idiopathic Silver-Russell syndrome (SRS): the SRS phenotype overlaps with the 12q14 microdeletion syndrome. J Med Genet 47: 356–360.
13. Fuke-Sato T, Yamazawa K, Nakabayashi K, Matsubara K, Matsuoka K, et al. (2012) Mosaic upd(7)mat in a patient with Silver-Russell syndrome. Am J Med Genet A 158A: 465–468.
14. Netchine I, Rossignol S, Dufourg MN, Azzi S, Rousseau A, et al. (2007) 11p15 imprinting center region 1 loss of methylation is a common and specific cause of typical Russell-Silver syndrome: clinical scoring system and epigenetic-phenotypic correlations. J Clin Endocrinol Metab 92: 3148–3154.
15. Kagami M, Yamazawa K, Matsubara K, Matsuo N, Ogata T (2008) Placentomegaly in paternal uniparental disomy for human chromosome 14. Placenta 29: 760–761.
16. Bell AC, Felsenfeld G (2000) Methylation of a CTCF-dependent boundary controls imprinted expression of the Igf2 gene. Nature 405: 482–485.
17. Hark AT, Schoenherr CJ, Katz DJ, Ingram RS, Levorse JM, et al. (2000) CTCF mediates methylation-sensitive enhancer-blocking activity at the H19/Igf2 locus. Nature 405: 486–489.
18. Takai D, Gonzales FA, Tsai YC, Thayer MJ, Jones PA (2001) Large scale mapping of methylcytosines in CTCF-binding sites in the human H19 promoter and aberrant hypomethylation in human bladder cancer. Hum Mol Genet 10: 2619–2626.
19. Fisher AM, Thomas NS, Cockwell A, Stecko O, Kerr B, et al. (2002) Duplications of chromosome 11p15 of maternal origin result in a phenotype that includes growth retardation. Hum Genet 111: 290–296.
20. Brena RM, Auer H, Kornacker K, Hackanson B, Raval A, et al. (2006) Accurate quantification of DNA methylation using combined bisulfite restriction analysis coupled with the Agilent 2100 Bioanalyzer platform. Nucleic Acids Res 34: e17.
21. Yamazawa K, Nakabayashi K, Kagami M, Sato T, Saitoh S, et al. (2010) Parthenogenetic chimaerism/mosaicism with a Silver-Russell syndrome-like phenotype. J Med Genet 47: 782–785.
22. Shaffer LG, Agan N, Goldberg JD, Ledbetter DH, Longshore JW, et al. (2001) American College of Medical Genetics statement on diagnostic testing for uniparental disomy. Genet Med 3: 206–211.
23. Hannula K, Lipsanen-Nyman M, Kontiokari T, Kere J (2001) A narrow segment of maternal uniparental disomy of chromosome 7q31-qter in Silver-Russell syndrome delimits a candidate gene region. Am J Hum Genet 68: 247–253.
24. Eggermann T, Schonherr N, Jager S, Spaich C, Ranke MB, et al. (2008) Segmental maternal UPD(7q) in Silver-Russell syndrome. Clin Genet 74: 486–489.
25. Begemann M, Spengler S, Kordass U, Schroder C, Eggermann T (2012) Segmental maternal uniparental disomy 7q associated with DLK1/GTL2 (14q32) hypomethylation. Am J Med Genet A 158A: 423–428.
26. Yamazawa K, Ogata T, Ferguson-Smith AC (2010) Uniparental Disomy and Human Disease: An Overview. Am J Med Genet C 154C: 329–334.
27. Gicquel C, Rossignol S, Cabrol S, Houang M, Steunou V, et al. (2005) Epimutation of the telomeric imprinting center region on chromosome 11p15 in Silver-Russell syndrome. Nat Genet 37: 1003–1007.
28. Bliek J, Terhal P, van den Bogaard MJ, Maas S, Hamel B, et al. (2006) Hypomethylation of the H19 gene causes not only Silver-Russell syndrome (SRS) but also isolated asymmetry or an SRS-like phenotype. Am J Hum Genet 78: 604–614.
29. Ulaner GA, Yang Y, Hu JF, Li T, Vu TH, et al. (2003) CTCF binding at the insulin-like growth factor-II (IGF2)/H19 imprinting control region is insufficient to regulate IGF2/H19 expression in human tissues. Endocrinology 144: 4420–4426.
30. Pham NV, Nguyen MT, Hu JF, Vu TH, Hoffman AR (1998) Dissociation of IGF2 and H19 imprinting in human brain. Brain Res 810: 1–8.
31. Albrecht S, Waha A, Koch A, Kraus JA, Goodyer CG, et al. (1996) Variable imprinting of H19 and IGF2 in fetal cerebellum and medulloblastoma. J Neuropathol Exp Neural 55: 1270–1276.
32. Kotzot D (2008) Maternal uniparental disomy 7 and Silver-Russell syndrome - clinical update and comparison with other subgroups. Eur J Med Genet 51: 444–451.
33. Kotzot D, Balmer D, Baumer A, Chrzanowska K, Hamel BC, et al. (2000) Maternal uniparental disomy 7-review and further delineation of the phenotype. Eur J Pediatr 159: 247–256.
34. Robinson WP (2000) Mechanisms leading to uniparental disomy and their clinical consequences. Bioessays 22: 452–459.
35. Hao Y, Crenshaw T, Moulton T, Newcomb E, Tycko B (1993) Tumour-suppressor activity of H19 RNA. Nature 365: 764–767.
36. Juan V, Crain C, Wilson C (2000) Evidence for evolutionarily conserved secondary structure in the H19 tumor suppressor RNA. Nucleic Acids Res 28: 1221–1227.
37. Arima T, Kamikihara T, Hayashida T, Kato K, Inoue T, et al. (2005) ZAC, LIT1 (KCNQ1OT1) and p57KIP2 (CDKN1C) are in an imprinted gene network that may play a role in Beckwith-Wiedemann syndrome. Nucleic Acids Res 33: 2650–2660.
38. Varrault A, Gueydan C, Delalbre A, Bellmann A, Houssami S, et al. (2006) Zac1 regulates an imprinted gene network critically involved in the control of embryonic growth. Dev Cell 11: 711–722.
39. Quenneville S, Verde G, Corsinotti A, Kapopoulou A, Jakobsson J, et al. (2011) In embryonic stem cells, ZFP57/KAP1 recognize a methylated hexanucleotide to affect chromatin and DNA methylation of imprinting control regions. Mol Cell 44: 361–372.
40. Yamazawa K, Nakabayashi K, Matsuoka K, Masubara K, Hata K, et al. (2011) Androgenetic/biparental mosaicism in a girl with Beckwith-Wiedemann syndrome-like and upd(14)pat-like phenotypes. J Hum Genet 56: 91–93.
41. Huang J, Lin Y, Li L, Qing D, Teng XM, et al. (2009) ARHI, as a novel suppressor of cell growth and downregulated in human hepatocellular carcinoma, could contribute to hepatocarcinogenesis. Mol Carcinog 48: 130–140.
42. Feng W, Marquez RT, Lu Z, Liu J, Lu KH, et al. (2008) Imprinted tumor suppressor genes ARHI and PEG3 are the most frequently down-regulated in human ovarian cancers by loss of heterozygosity and promoter methylation. Cancer 112: 1489–1502.
43. Tang HL, Hu YQ, Qin XP, Jazag A, Yang H, et al. (2012) Aplasia ras homolog member I is downregulated in gastric cancer and silencing its expression promotes cell growth in vitro. J Gastroenterol Hepatol 27: 1395–1404.
44. Blyth M, Huang S, Maloney V, Crolla JA, Karen Temple I (2008) A 2.3 Mb deletion of 17q24.2-q24.3 associated with 'Carney Complex plus'. Eur J Med Genet 51: 672–678.
45. Midro AT, Debek K, Sawicka A, Marcinkiewicz D, Rogowska M (1993) Second observation of Silver-Russel syndrome in a carrier of a reciprocal translocation with one breakpoint at site 17q25. Clin Genet 44: 53–55.
46. Dörr S, Midro AT, Farber C, Giannakudis J, Hansmann I (2001) Construction of a detailed physical and transcript map of the candidate region for Russell-Silver syndrome on chromosome 17q23-q24. Genomics 71: 174–181.
47. Cuomo CA, Kirch SA, Gyuris J, Brent R, Oettinger MA (1994) Rch1, a protein that specifically interacts with the RAG-1 recombination-activating protein. Proc Natl Acad Sci U S A 91: 6156–6160.

48. Weis K, Mattaj IW, Lamond AI (1995) Identification of hSRP1 alpha as a functional receptor for nuclear localization sequences. Science 268: 1049–1053.
49. Dörr S, Schlicker M, Hansmann I (2001) Genomic structure of karyopherin alpha2 (KPNA2) within a low-copy repeat on chromosome 17q23-q24 and mutation analysis in patients with Russell-Silver syndrome. Hum Genet 109: 479–486.
50. Matsubara K, Murakami N, Nagai T, Ogata T (2011) Maternal age effect on the development of Prader-Willi syndrome resulting from upd(15)mat through meiosis 1 errors. J Hum Genet 56: 566–571.

RESEARCH ARTICLE

AMERICAN JOURNAL OF medical genetics PART B
Neuropsychiatric Genetics

A Loss-of-Function Mutation in the *SLC9A6* Gene Causes X-Linked Mental Retardation Resembling Angelman Syndrome

Yumi Takahashi,[1] Kana Hosoki,[1] Masafumi Matsushita,[2] Makoto Funatsuka,[3] Kayoko Saito,[4] Hiroshi Kanazawa,[2] Yu-ichi Goto,[5] and Shinji Saitoh[1]*

[1]Department of Pediatrics, Hokkaido University Graduate School of Medicine, Sapporo, Japan

[2]Deparrtment of Biological Sciences, Graduate School of Science, Osaka University, Osaka, Japan

[3]Department of Pediatrics, Tokyo Womens' Medical University, Tokyo, Japan

[4]Institute of Medical Genetics, Tokyo Womens' Medical University, Tokyo, Japan

[5]Department of Mental Retardation and Birth Defect Research, National Institute of Neuroscience, National Center of Neurology and Psychiatry, Tokyo, Japan

Received 29 November 2010; Accepted 6 July 2011

SLC9A6 mutations have been reported in families in whom X-linked mental retardation (XMR) mimics Angelman syndrome (AS). However, the relative importance of *SLC9A6* mutations in patients with an AS-like phenotype or XMR has not been fully investigated. Here, the involvement of *SLC9A6* mutations in 22 males initially suspected to have AS but found on genetic testing not to have AS (AS-like cohort), and 104 male patients with XMR (XMR cohort), was investigated. A novel *SLC9A6* mutation (c.441delG, p.S147fs) was identified in one patient in the AS-like cohort, but no mutation was identified in XMR cohort, suggesting mutations in *SLC9A6* are not a major cause of the AS-like phenotype or XMR. The patient with the *SLC9A6* mutation showed the typical AS phenotype, further demonstrating the similarity between patients with AS and those with *SLC9A6* mutations. To clarify the effect of the *SLC9A6* mutation, we performed RT-PCR and Western blot analysis on lymphoblastoid cells from the patient. Expression of the mutated transcript was significantly reduced, but was restored by cycloheximide treatment, indicating the presence of nonsense mediated mRNA decay. Western blot analysis demonstrated absence of the normal NHE6 protein encoded for by *SLC9A6*. Taken together, these findings indicate a loss-of-function mutation in *SLC9A6* caused the phenotype in our patient.

Key words: *SLC9A6*; sodium/hydrogen exchanger 6; Angelman syndrome; X-linked mental retardation; nonsense mediated mRNA decay

How to Cite this Article:
Takahashi Y, Hosoki K, Matsushita M, Funatsuka M, Saito K, Kanazawa H, Goto Y-I, Saitoh S. 2011. A Loss-of-Function Mutation in the *SLC9A6* Gene Causes X-Linked Mental Retardation Resembling Angelman Syndrome.
Am J Med Genet Part B 156:799–807.

INTRODUCTION

SLC9A6 mutations were first reported by Gilfillan et al. [2008] in families exhibiting an X-linked mental retardation (XMR) syndrome mimicking Angelman syndrome (AS). Angelman syndrome is characterized by severe developmental delay with absent or minimal speech, ataxia, easily provoked laughter, epilepsy, and microcephaly. The syndrome is caused by loss-of-function of the *UBE3A* gene which is subject to genomic imprinting. Patients with *SLC9A6* mutations resemble patients with AS, but also demonstrate distinctive clinical features including cerebellar atrophy, slow progression of symptoms, increased glutamate/glutamic acid peak on magnetic resonance spectroscopy (MRS), and lack of characteristic abnormalities seen AS patients examined using electroencephalography (EEG). Following the first report in 2008, in 2010 Schroer et al. reported two other families with AS due to *SLC9A6* mutations, and confirmed the findings of Gilfillan et al.

The *SLC9A6* gene is located on Xq26.3, and encodes the ubiquitously expressed Na^+/H^+ exchanger protein member 6, NHE6. The NHE protein family consists of nine members and includes

Grant sponsor: Ministry of Education, Culture, Sports, Science, and Technology, Japan; Grant number: 21591306.
*Correspondence to:
Shinji Saitoh, Department of Pediatrics, Hokkaido University Graduate School of Medicine, N-15, W-7, Kita-ku, Sapporo 060-8638, Japan.
E-mail: ss11@med.hokudai.ac.jp
Published online 2 August 2011 in Wiley Online Library (wileyonlinelibrary.com).
DOI 10.1002/ajmg.b.31221

NHE1-5 which is found in the plasma membrane, and NHE6-9 which is found in the membranes of intracellular organelles such as mitochondria and endosomes. NHE6 is predominantly present in the early recycling endosome membranes, and is believed to have a role in regulating luminal pH and monovalent cation concentration in intracellular organelles [Brett et al., 2002; Nakamura et al., 2005]. Moreover, Roxrud et al. demonstrated that NHE6 in combination with NHE9 participated in regulation of endosomal pH in HeLa cells by means of the procedure of co-depletion of NHE6 and NHE9 [Roxrud et al. 2009], indicating the significant role of NHE6 in fine-tuning of endosomal pH in human cells. In the brain, exocytosis from recycling endosomes is essential for the growth of dendritic spines which grow during long-term potentiation (LTP). In the absence of recycling endosomal transport, spines are rapidly lost, and LTP stimuli fail to elicit spine growth [Park et al., 2006]. Thus, NHE6 has an important role in the growth of dendritic spines, and also in the development of normal brain wiring. Thus far, five *SLC9A6* mutations have been reported in six AS families; two nonsense mutations, one inframe deletion, one frameshift deletion, and one splicing mutation [Gilfillan et al., 2008; Schroer et al., 2010]. The precise pathogenesis by which these mutations produce disease remains to be clarified.

The aim of this study was to clarify the incidence and importance of *SLC9A6* mutations in AS-like patients and patients with XMR, and to shed light on the molecular pathogenesis of disease due to *SLC9A6* mutations.

MATERIALS AND METHODS

Enrolled Patients

We examined 22 affected Japanese males clinically suspected of having AS but who lacked the genetic abnormalities reported in AS (AS-like cohort). These patients had AS excluded by having negative results for the *SNURF-SNRPN* DNA methylation test (which identifies a deletion, uniparental disomy, or imprinting defect) and *UBE3A* mutation screening (performed as described previously) [Saitoh et al., 2005]. We also examined DNA samples from 104 Japanese patients suspected of having XMR (XMR cohort). The XMR samples were collected as a part of a project for the Japanese Mental Retardation Consortium [Takano et al., 2008]. This study was approved by the Institutional Review Board of Hokkaido University Graduate School of Medicine, and written informed consent was obtained from the parents of the enrolled patients.

Mutation Analysis of the *SLC9A6* Gene

We amplified each exon, including exon–intron boundaries, of the *SLC9A6* gene using polymerase chain reaction (PCR), and all amplicons were directly sequenced on an ABI 3130 DNA analyzer (Applied Biosystems, Foster City, CA) using BigDye Terminator V.1.1 Cycle Sequencing Kit (Applied Biosystems). *SLC9A6* encodes two alternatively spliced transcripts produced from alternative splicing donor sites in exon 2 which give rise to a long form designated as variant 1, and a short form called variant 2. Variant 1 and variant 2 code for NHE6.1 (isoform a) and NHE6.0 (isoform b), respectively (Fig. 1). The primers were designed to amplify each transcript variant. The primers sequence used for amplification and sequencing are available on request. Genomic DNA (10 ng) extracted from peripheral blood was amplified in a total PCR volume of 20 μl containing 1× buffer, 0.4 μM of each primer (forward/reverse), 0.18 mM dNTPs, 0.5 U AmpliTaq Gold® DNA Polymerase (Applied Biosystems). The PCRs for all exons except exon one were performed at 94°C for 10 min followed by 30 cycles of 94°C for 30 sec, 55°C for 30 sec, 72°C for 30 sec, then one cycle at 72°C for 7 min. The high CpG content of exon 1 required it to be amplified in a total reaction volume of 20 μl containing 1× buffer, 0.4 μM of each primer, 0.2 mM dNTPs, 0.4 U Phusion® Hot Start High-Fidelity DNA Polymerase (Finnzymes, Vantaa, Finland), and 3% DMSO. The thermocycling conditions for exon 1 were 98°C for 3 min followed by 35 cycles of 98°C for 10 sec, 65°C for 30 sec and 72°C for 30 sec and then one cycle of 72°C for 5 min. The PCR products were purified with Wizard® PCR Preps DNA Purification System (Promega, Madison, WI) prior to sequencing. All mutations are referred to in relation to reference sequence NM_001042537.

Cell Culture and Cycloheximide Treatment

Epstein–Barr virus (EBV)-transformed lymphoblastoid cells lines were established from peripheral blood cells using standard methods. To prevent potential degradation of transcripts containing premature translation termination codons (PTCs) by nonsense mediated mRNA decay (NMD), lymphoblastoid cells from the patient with the *SLC9A6* mutation and normal controls were treated with 100 μg/ml cycloheximide (CHX) (Sigma, St. Louis, MO). This compound interferes with NMD through inhibition of protein synthesis [Aznarez et al., 2007]. CHX or a 0.1% DMSO control vehicle was used 4 hr prior to RNA extraction from the cell lines [Carter et al., 1995].

RT-PCR

Total RNA from cultured lymphoblastoid cells from the patient and four normal controls, was extracted using the RNAqueous® Kit (Applied Biosystems). Reverse transcription was performed using 100 ng of total RNA and the High-Capacity cDNA Reverse Transcription Kit (Applied Biosystems) in a total reaction volume of 20 μl containing 1× Random primers, 4 mM dNTP mix, 2.5 U of Multiscribe™ Reverse Transcriptase, and 1 μl of RNase Inhibitor. The reactions were incubated at 25°C for 10 min, then at 37°C for 120 min and then followed by 85°C for 5 min to inactivate the reverse transcriptase. Complementary DNA was then amplified using a primer set designed to amplify exon 2–5; forward 5′-GTCTTTTGGTGGGCCTTGT-3′, reverse 5′-GTCCCGTTACC-TTCATCAG-3′. PCR products for NHE6.1 (transcript variant 1) and NHE6.0 (transcript variant 2) were 399 and 303 bp, respectively.

Real-Time Quantification of *SLC9A6* mRNA

To measure *SLC9A6* transcript variant 1 and variant 2, both of which are alternative splicing products, primers and TaqMan® MGB probes were designed with Primer® Express Software (Applied Biosystems; Fig. 1). The Primer and MGB probe sequence

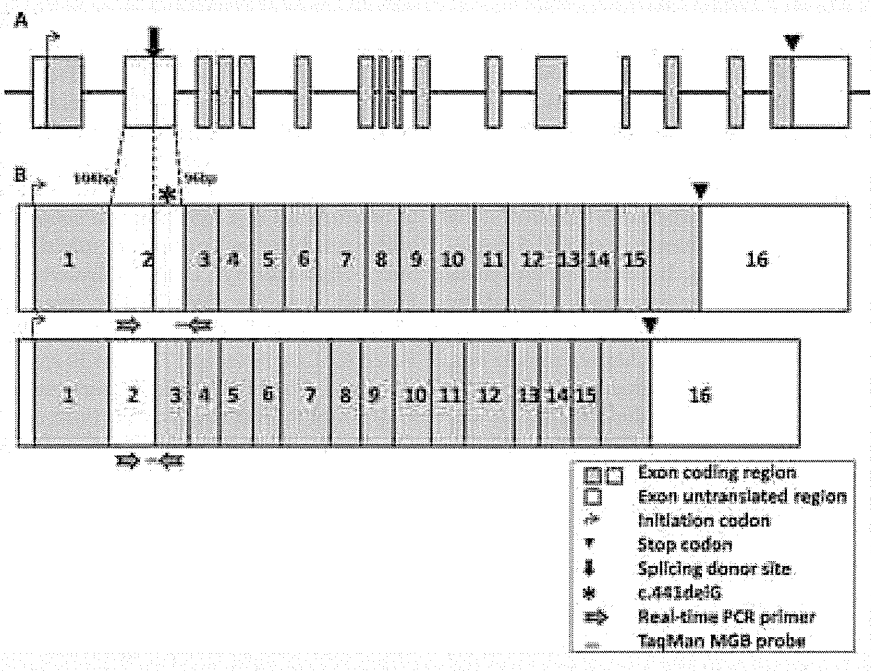

FIG. 1. A: Genomic structure of the *SLC9A6* gene. B: Two alternatively spliced transcripts of the *SLC9A6* gene. Above: *SLC9A6* transcript variant 1 (encodes NHE6.1 or isoform a). Below: *SLC9A6* transcript variant 2 (encodes NHE6.0 or isoform b). The location of the *SLC9A6* mutation in our patient is shown with *. Primers and probes used in real-time quantitative PCR are shown (horizontal arrows).

for variant 1 were forward primer 5′-TGAGTATATGCTGAAAGGAGAGATTAGTTC-3′, reverse primer 5′-GATAGGAGGAAGTAATATGTTGAAAAATACTTC-3′, TaqMan MGB probe 5′-CTTAGAAAGGTTACTTTTGATCC-3′; and for variant 2 forward primer 5′-CTGTGAAGTGCAGTCAAGTCCAA-3′, reverse primer 5′-GATAGGAGGAAGTAATATGTTGAAAAATACTT-3′, TaqMan MGB probe 5′-CTACCTTACTGGTTACTTTTGA-3′. Human *GAPDH* MGB probe and primers purchased from Applied Biosystems were used as the internal control. Patient cDNA was transcribed from 10 ng of total RNA in a total volume of 25 μl containing 1× TaqMan® Universal PCR Master Mix (Applied Biosystems), 0.9 μM of each primer (sense/antisense) and 0.25 μM of probe. Thermocycling was 95°C for 10 min, followed by 40 cycles of 95°C for 15 sec and 60°C for 1 min. Real-time quantitative PCR was performed using the ABI PRISM 7700 (Applied Biosystems). The $2^{-\Delta\Delta Ct}$ method was used for relative quantification.

Western Blot Analysis

HeLa cells and cultured lymphoblastoid cells from the patient, mother and normal controls were washed with phosphate buffered saline and suspended in lysis buffer (phosphate buffered saline containing 1% Triton-X, 1 μg/ml aprotinin, 1 μg/ml pepstatin A, and 1 μg/ml leupeptin). HeLa cells expressing the NHE6.1 were used as a control. The cells were disrupted by sonication and centrifuged at 20,000*g* for 10 min at 4°C. The supernatants were then resolved by SDS-polyacrylamide electrophoresis and transferred to polyvinylidene fluoride membrane (Millipore, Billerica, MA). NHE6 was detected with rabbit polyclonal anti-NHE6 antibody [Ohgaki et al., 2008], anti-rabbit IgG antibody conjugated with horseradish peroxidase (Vector Laboratories, Burlingame, CA) and chemiluminescence reagent (ECL Western Blotting Detection System; GE Healthcare, Waukesha, WI).

RESULTS

Identification of a *SLC9A6* Mutation

We identified only one male patient with a frameshift mutation (c.441delG, p.S147fs) in exon 2, out of 22 male patients in the AS-like cohort (Fig. 2). This frameshift mutation causes a PTC. His healthy mother was heterozygous for the mutation.

No mutation in the *SLC9A6* gene was identified in the XMR cohort. However, two common polymorphisms (rs2291639, rs2307131), and one putative novel polymorphism in intron 12 (c.1692 +10 A>G) were detected.

Clinical Features of the Patient With the *SLC9A6* Mutation

The affected male patient at birth suffered from mild neonatal asphyxia, however he had no other perinatal problems. His parents